COMPARATIVE STUDY OF NiO-ZnO (NZ) AND CuO-ZnO (CZ) COMPOSITE NANOFIBERS FOR POTENTIAL APPLICATION IN WATER REMEDIATION

A DISSERTATION

Submitted in partial fulfilment of the requirements for the award of the degreeof

MASTER OF TECHNOLOGY

in

BIOPROCESS ENGINEERING

by

VIKASH KUMAR

DEPARTMENT OF BIOTECHNOLOGY

INDIAN INSTITUTE OF TECHNOLOGY ROORKEE
ROORKEE – 247 667 (INDIA)
MAY, 2019

COMPARATIVE STUDY OF NiO-ZnO (NZ) AND CuO-ZnO (CZ) COMPOSITE NANOFIBERS FOR POTENTIAL APPLICATION IN WATER REMEDIATION

A DISSERTATION

Submitted in partial fulfilment of the requirements for the award of the degreeof

MASTER OF TECHNOLOGY

in

BIOPROCESS ENGINEERING

by

DEPARTMENT OF BIOTECHNOLOGY

INDIAN INSTITUTE OF TECHNOLOGY ROORKEE

ROORKEE-247 667 (INDIA)

MAY, 2019

CANDIDATE'S DECLARATION

I hereby declare that the work presented in dissertation entitled**“”**submitted in partial fulfillment of the requirements for the award of degree of **Master of Technology** in **Bioprocess engineering**, **Indian Institute of Technology Roorkee**, is an authentic record of my work carried out under thesupervision of **Dr. P. Gopinath**, Associate Professor, Department of Biotechnology, IITRoorkee. The matterembodied in this work has not been submitted by me for the award of any otherdegree.

Vikash kumar
Enrolment No. 17559008
Date:

CERTIFICATE

This is to certifythat the above statement made by the candidate is correct to the best of my knowledge.

Dr. P. Gopinath
Supervisor
Associate Professor
Department of Biotechnology
Indian Institute of Technology Roorkee

TABLE OF CONTENTS

LIST OF FIGURES

LIST OF TABLES

ABBREVIATIONS

%.....	Percentage
Cu…….	Copper
CuO……..	Copper oxide
DMF……..	Dimethylformamide
Ni	Nickel
NiO	Dubinin - Radushkevich
Zn…….	Zinc
ZnO……	Zinc oxide
NiO-ZnO……	Nickel oxide-Zinc oxide
NZ……..	Nickel oxide-Zinc oxide composite nanofiber
CuO-ZnO……...	Copper oxide- Zinc oxide
CZ ……..	Copper oxide- Zinc oxide composite nanofiber
FESEM…….	Field emission scanning electron microscope
FTIR……..	Fourier Transform Infrared Spectroscopy
g…….	Gram
h…….	Hour
HRTEM……	High resolution transmission electron microscope
JCPDS……	Joint Committee on Powder Diffraction Standards
K……	Kelvin
k ……	First order rate constant
k_2……	Second order rate constant
KeV……	Kilo electron volts
K_F……...	Freundlich adsorption constant
PAN……...	Polyacrylonitrle
K_L……...	Langmuir adsorption constant
$CuAc_2$……..	Copper acetate
$ZnAc_2$…….	Zinc acetate
$NiAc_2$……..	Nickel acetate
XRD……	X-ray diffraction

XPS	X-ray photoelectron spectroscopy
min…….	Minute
µL……..	Micro litre
µg……...	Microgram
mg……..	Milligram
nm……..	Nanometer
NPs…….	Nanoparticles
O.D…….	Optical Density
NC……	Nanocomposite
PAN……	Polyacrylonitrile
q_{eq}……..	Equilibrium adsorption capacity
q_m……..	D-R monolayer adsorption capacity
q_{max}…….	Maximum adsorption capacity
ROS…….	Reactive Oxygen Species
rpm…….	Rotation per minute
s……..	Seconds
SAED…….	Selected area electron diffraction
t……..	Time
TEM……...	Transmission electron microscope
TG/DTA……	Thermogravimetric/Differential thermal analysis
UV……..	Ultraviolet

Acknowledgements

I want to thanks to my advisor, Dr P.Gopinath for his confident on me and given this research platform for enhancement of my career forward. I thank him for his undeterred support, guidance and motivation which encouraged me to achieve this milestone. Under his guidance, I had obtained enormous freedom to think over innovative ideas, conceptions and new perspectives for finding solutions to the problems. His ardent dedication, hard work and activeness has been the source of inspiration to me and many more around him. His timely decisions at the moment of hardships and deadlines were priceless. Thank you very much once again for this wonderful journey and I eagerly look forward for the future expeditions down the lane.

My sincere thank goes to Raj Kumarsir, his guidance and generous advice helped in all the time of resources and writing of the thesis, I would to thank my friend Madhulika Narayan for her endless support, encouragement and valuable suggestions. I would also like tothank Chokulingum, Shanid, Vinay, Shlock, Sandeep, Mehak and other lab matesfor their continuously guidance and support during the thesis work.

I extend my sincere thanks to the heads of the Centre of nanotechnology and biotechnology department during my period of stay, Prof. R. K. Dutta, and Prof.A.K.sharma respectively for timely support and constructive ideas. I am highly obliged to express my sincere thanks other faculties , Dr.souravDatta, Dr. Sanjay Ghosh , Dr.Bijan and Dr.Majumdarfor their valuable their guidance . Moreover, it would be incomplete without acknowledging the technical staffs of IIC who has been the vital support throughout my research work, I specially thank them all for their kind and prompt response whenever required.

It would have not been possible without my family who encourage and given me support throughout my thesis. I would to extend to heartfelt thanks to all my classmates of Bioprocess engineering specially Nikhil, Pawan, Vikrant ,Nishikant and Nayan for supporting and taking an active interest in project life.

I extend my sincere thanks to the staffs of Centre of Nanotechnology Mr. Rawan Pal, Mr. Vinod, Mr. Naresh and Mr. Riyaz for lending kind help in their own respective means. Thank you for your cheerful speeches and cracking of jokes that makes me happy

Abstract

The comparative study of NiO-ZnO (NZ) and CuO-ZnO(CZ) composite nanomaterials was investigated for photocatalytic and adsorption applicationin order to remove the Congo red (CR) dye in presence and absence of visible light. Both NZ and CZ composite nanomaterials have been fabricated by electrospinning followed by heat treatment techniques calcination. The products were characterized using X-Ray Diffraction (XRD), Fourier Transform Infra-Red (FTIR)andFESEM(field emission scanning electron microscopic), TGA (thermo gravimetric analysis), HR-TEM (High resolution transmission electron microscope), DRS (diffusion reflectance spectroscopy), XPS (photo luminance study) for their morphological and structural details. The photocatalytic experiments were conducted for the degradation of CR dye under solar irradiationIt was found that reactions followed first order kinetics from which the rate constants were determined .Adsorption study has done for CR removal in two cases with shaking(rpm=200) and without shaking. Adsorption isothermand kinetics study has been performed and it was found for isotherm , Freundlich model best fitted to data and pseudo second order were following the adsorption kinetics. The experimental results revealed thatin presence of sunlight CZ showed quite similar removal efficiency of dye than NZ, but in absence of sunlight NZ were displayeda better removal efficiency of dye.

CHAPTER 1 INTRODUCTION

1.1 Introduction

It is predicted that population of world will be nine billion by 2050. It will stress already limited water supply. Industries and urbanization growing very fast and it is putting a lot of stress on drinking water. Industries effluent contains harmful heavy metals (mercury, cobalt, lead etc.) organic and inorganic substances ; these substances are very toxic to aquatic as well as for human life if somehow they come in contact(Puvaneswari et al., 2006).

Dyes are widely used in textile industry, paper industry andfor laboratory purpose. But dyes are very toxic and carcinogenic in nature. It can cause several types of cancer and skin problems.It is also a major concern for aquatic life. The current technologies available for removal of dye are electrolysis, flocculation, ozonation , membrane filtration. But these technologies are less effective and very expensive. Therefore there is need to developed the technologies which can be inexpensive and effective. These days nanomaterialsare looking more promising since it has high surface area to volume ratio, high porosity and continuous structure`(Indexed et al., 2018).

Currently photo catalyst has gained attention. It has potential to degrade the dye in a few hour depending upon the dye concentration(Afkhami and Moosavi, 2010). It does not need any power supply; it can simply utilize the sunlight to degrade the dye(Choksumlitpol et al., 2017).

Metal oxides such as ZnO_2, SnO_2,CuO,TiO_2 exit abundance in nature band gap ranging from 1eV to 3 eV which enable to use them as semiconductors(Yin et al., 2005). In presence of sunlight due to electron-holes movement reactive oxygen species (ROS) forms. ROSs havepotential to degrade the different type of organic dyes and it can inactivate various pathogenic microorganism.

In this work we successfully synthesize NiO-ZnO and CuO-ZnO nanocomposite fibersmetal oxides by simple electrospinning and calcination process., after that compared their characteristics and efficiency in adsorption and photocatalytic process. It is known from literature NiO and CuOmetal oxide are p-type semiconductor, whereasZnOis n-type semiconductor. In this study,ZnO coupled with NiO and CuO respectively to form p-n type

semiconductor. These nanomaterials are capable of degrading the dye in presence of sunlight. Moreover they have large surface area so that their adsorption capacity is high.

1.2 Objectives

The key objectives of the present work are as follows

- Fabrication and development of two different PAN templated metal oxidenanocomposites (NCs)by combining electrospinning technique and calcination.
- Characterization of the NCsusing various analytical techniques.
- Investigation of photocatalytic degradation properties of Nickel oxide/Zinc oxide (NZ) and Copper oxide/Zinc oxide (CZ) (NCs) using congo red as model dye under sunlight irradiation.
- Investigation of adsorption properties of both NCs using CR dye with and without mechanical agitation (orbital shaker).
- Batch adsorption experiments i.e. kinetics studies and isothermal studiesto investigate the adsorption process.
- Comparative analysis and observations.

1.3Significance of the present study

The significance and salient features of the present work has been summarized below.

- In this work two different polymeric/metal oxide blend solutions were prepared and electrospun to form two different type of nanofibers and has been calcined in order to obtain polymeric nanocomposites (NCs).
- Further the two nanocomposites i.e. CZ and NZ NCs were utilized for conducting various batch experiments and compared its dye removal properties.
- Initially the NCs were used to investigate the photocatalytic properties under sunlight irradiation and comparative analysis was performed.
- Simultaneously, the adsorption properties of the same NCs were studied by conducting batch adsorption experiments and the results were discussed.
- This work is the first of its kind that the synthesized nanocomposites were studied for both the photocatalytic properties and adsorption properties.

- The results found that the nanocomposites which are effective in the sunlight mediated photocatalytic degradation, also removes dyes from the aqueous solutions through adsorption process.
- From the findings, it was postulated that the comparative analysis of nanocomposites gives insightful information related to the dual properties of the hybrid nanomaterials

CHAPTER 2 LITRATURE REVIEW

2.1. Nanofiber

Nanofibers have gained wide attention and it has several features including high surface area to volume ratio, high porosity making it has wide range of applications(Gao et al., 2013). Some of applications are synthetic polymers and nanocomposites polymers. Nanomaterial widely using in water remediation , health care, energy generation, photo catalytic degradation and adsorption(Nasreen et al., 2019).

Nanofiber can be prepared by three methods: phase separation, self-assembly and electrospinning as following:

Phase separation technique widely used to make three dimensions scaffold, in phase separation technique there are two domain phase get separated by adding a non-polymer solvent (non – solvent) or changing the temperature (thermally induced). The drawback of that technique it cannot be scale up.

In self-assemblynanoparticle can be formed and organized into the structure by providing temperature gradient or other constraint. But it is very difficult to characterize.

Third method for the preparation of fiber is electrospinning(Huang et al., 2003), it has gained much attention due to ability to electro spun wide variety of polymer and it is very simple and cost effective technique. Electrospinning is a very useful technique formaking polymeric nanofiber which utilize the electrostatic interaction to produce the nanofiber.

This is very robust and simple technique it can spin variety of polymers in order to make nanofiber which have several characteristics including high surface area to volume ratio, high porosity. These fibers are versatileand having a wide range of applications such as filtration, drugs delivery, biosensors and biological scaffold.

The term “electrospinning” derived from “electrostatic spinning” itdefinesas it can spin the variety of polymer solution by electrostatic force(Purushothaman et al., 2019).

2.2 Principle of electrospinning

Electrospinning is an unique approach to obtained the continues ultrathin nanofiber which have high surface area and porosity. In this technique voltage of several kV is necessary to generate. In the electrospinning process, a polymer solution held by its surface tension at the end of capillary tube. When electric field applied by increasing voltage there is liquid charge induced on the polymer droplet(Teck, 2017). When the applied field attains the critical value then repulsive force overcome on the surface tension as a result there is morphological change in droplet and ejection of charge jet from Taylor cone and the charged jet can be collected on collector(Malwal and Gopinath, 2016).

2.3 Effect of various parameter on electrospinning

2.3.1 Solution parameters

(A)Concentration

There should be optimum concentration have to maintained in order to form desired size of fibers. At low concentration beads forms instead of fiber, when concentration increase above the optimum large and nonuniform fibers forms which is not desirable(Thavasi et al., 2008).

(B) Molecular weight

Molecular weight of the polymer playsan important role in viscosity of solution. If molecular weight of polymer is low, it tends to form beads rather than fiber. On the other hand if polymer weight is high it leads to form large diameter fibers.

(C) Surface tension

Viscosity lower the surface tension of solvent suitable for electrospinning because it help electrospinning to occur at lower electric field. However, it is not always essential lower surface tension always fit the electrospinning.

(D) Conductivityit was observed that when the conductivity of solution is high, smaller diameter are formed. Therefore conductivity should be maintained according to desirable size of fibers(Mahmood et al., 2011).

2.3.2Processing parameter

1) **Voltage**

   There is a lot of dispute on effect of voltage on size of fibers. Some researchers have observed when high voltage is applied the more polymer solution comes out through the syringe therefore large diameter formation take place. Some author was find out increasing applied voltage increase the repulsive force on the droplets which favors the narrowing of fibers diameter

2) **Flow rate**

   it was seen with increasing the flowrate diameter of fibers increased and normally at high flow rates beads are forms due to not able to get sufficient for drying before it reaches to collector.

3) **Tip to collector distance**

   It was observed that distance between the tip and collector affect the morphology of fiber. Minimum distance give fiber to enough time for drying before it reaches to the collector otherwise beads will form it is not provide sufficient time for drying.

2.4.2 Congo red dye

Congo red is the azo-dye , when it dissolve in water , the solution become reddish in color. In our experiment Congo red was taken as a model dye for adsorption as well as photocatalytic experiment(Afkhami and Moosavi, 2010). It is an organic dye, the sodium salt of 3,3′-([1,1′-biphenyl]-4,4′-diyl)bis(4-aminonaphthalene-1-sulfonic acid(Tan et al., 2011).

In photocatalytic reaction , photocatalyst produces ROS (reactive oxygen species) and it further cleave the structure CR dye to produce carbon dioxide and water molecule(Gao et al., 2014).

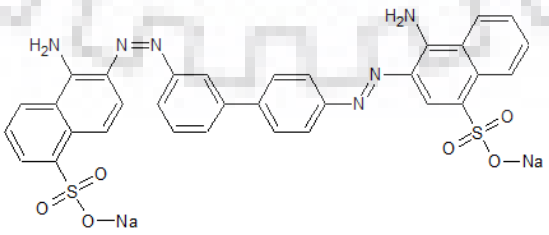

Fig2.4.2.: Structure of Congo red

2.4Metal oxides

2.4.1 Nickel oxide

Nickel oxide popularly use as p-type semiconductor material. It has band gap ranging from3.6 to 4.0 eV. It is very versatile metal oxides because it has high surface area to volume ratio and it has high adsorption capacity(El-Kemary et al., 2013). It can used easily for multimetal oxides which can be used as a photocatalyst for the degradation of dye in water remediation.

It has other application such as battery cathode, gas sensor and magnetic material. It has several other biomedical application(El-Kemary et al., 2013).

2.4.2 Copper oxide

A copper oxide (CuO) is an important transition metal oxide with monoclinic structure having a band gap 1.2 eV (indirect). Copper oxide is p- type semiconductor and it has wide range of application including photo catalyst biosensor, magnetic media and optical device batteries and catalyst(Dhineshbabu and Vetumperumal, 2016).

2.4.3 Zinc oxides

Zinc oxides widely used as semiconductor because it has wide range of band gap (3.44 eV at low temperature and 3.74 eV at room temperature) and it has many optoelectronics applications including laser diodes(Janotti and Walle, 2009), light emitting diode and photodetector

A) **Piazoelectric constant** – Zinc oxide has large piezoelectric constant when voltage is applied it leads to deformation in the ZnO crystal or vice versa.

B) Strong luminesce

Zinc oxide is n type semiconductor or it electron acceptor and it has strong luminescence enable it for application in fluorescent machine display(Gogoi et al., 2006).

C) **Thermal conductivity**

It has high thermal conductivity therefore it can add to rubber etc. to increase their thermal conductivity of the material. Zinc oxide widely used as photo catalyst because of their electronic configuration and light absorption properties.

2.5 Photocatalytic process and mechanism

When two semiconductor combine n type with p type it forms a junction which called p-n junction forms, therefore the electron start diffusing from n side to p side and holes start diffusing from p sides to n side until it reaches to equilibrium where it developed an electric field(Patiha et al., 2016). When light with certain energy strike on the heterogeneous it and it absorb the light with energy equal to higher than its band gap or threshold energy, itexits the electron and it start migrating towards valence band of p type semiconductor and holes diffuse towards the conduction band(Grandgirard et al., 2002). Holes combines with water molecule to form hydroxyl radicals (OH^-) and electron on the surface of photcatalyst react with dissolved oxygen to generate superoxide radicals ions (O_2^-) (Yu et al., 2006)which later forms hydroxyl radicals (OH^-) via generation of hydroxyl radicals(Malwal and Gopinath, 2017a).

Dye degradation mechanism

$h^+ + H_2O \rightarrow OH^{\cdot} + H^+$

$Dye + light \rightarrow Dye^*$

$Dye^* + heterostructure \rightarrow Dye^{\cdot+} heterostructure + e_{CB}^-$

$e_{CB}^- + O_2 \rightarrow O_2^{\cdot-}$

$Dye^{\cdot+} + O_2^{\cdot-} \rightarrow$ degradation products

ROSs ($^{\cdot}OH$, O_2^- ,$H_2O_2^{\cdot}$,$O_2^{\cdot}$), it has potential to degrade and inactivates various type of inorganic dyes and microorganism respectively(Bandekar et al., 2014).

ROSs can diffuse inside the microorganism through the cell wall and it can combine with their genomic material to inactivate the microbes.(Gogoi et al., 2006)

2.6 Adsorption process

There are numbers of technique present to remove the pollutant from the contaminated water, but adsorption is very popular among them because it is very efficient and economical

for water remediation. In adsorption liquid or gas adsorbed on the surface of solid(Malwal and Gopinath, 2017b). The solid that adsorbs the solute of liquid or gas called adsorbent and the component get adsorb is known as adsorbate. Molecules get adsorbed on the surface of solid because it has “affinity” to absorb on the surface of adsorbent. Adsorption process widely used in separation process in various industries like chemical and biotech etc.

On the basis of interaction process adsorption process can be divided into two types, if the interaction force weak between the adsorbent and adsorbate is called physisorption , it happen due to the vender Waal’s or electrostatic interaction. Furthermore if interaction force between them is strong then chemical bond can be formed called chemisorption.

Adsorption can be reversible and it is called desorption. In some cases adsorbed solute are desirable product and it can be recover by desorption process for example hydrocarbon from a gas stream.

There are two parameter which can affect the adsorption process are temperature and pressure. Adsorption favored at high pressure and lower temperature.

2.6.1 Characteristics and property of adsorbent

Since adsorbent has a very specific pore size so it allow specific molecule to diffuse inside the pore and depending on the size of adsorbate inside the pore therefore there rate can be vary. Selectivity due to difference in their rate of diffusion and adsorption is sometime called kinetic selectivity

Another factor is adsorption capacity, a good adsorbent must have capacity of adsorption capacity it depends on the surface of adsorbent (m^2/g) , if surface area is high . adsorptioncapacity may slowly decrease with on repeated use of adsorbent; therefore reversibility of adsorption comes into the picture where adsorbate remove from the adsorbent surface by varying some parameter for example pH, temperature etc.

The other important features of an adsorbent are :

(i) Porosity and pore size distribution

(ii) Structural strength stability

(iii) Particle size and its distribution

CHAPTER 3 MATERIALS AND METHODS

3.1 Materials

3.1.1 Reagents

- Congo Red (CR)(Mw = 696.68 g/mol)
- Copper acetate monohydrate ($CuAc_2$) [$Cu(CH_3COO)_2 . H_2O$] (Mw = 199.65 g/mol)
- N, N- Dimethylformamide (DMF) [C_3H_7NO] (Mw = 73.09 g/mol)
- Polyacrylonitrile (PAN) [$(C_3H_3N)n$] (Avg. Mw = 150,000)
- Ultrapure Water (18 MΩ)
- Zinc acetate dihydrate ($ZnAc_2$) [$Zn(CH_3COO)_2 . {}_2H_2O$] (Mw = 219.49 g/mol)
- Nickel(ll) acetate tetrahydrate($NiAc_2$)[$C_4H_{14}NiO_8$] (Mw = 248.841 g/mol)

3.1.2 Equipment

- Autoclave (NANOMAG)
- Electrospinning machine (ESPIN NANO, PECO)
- Fourier transform infrared spectrometer (FTIR) (Thermo Nicolet)
- Thermogravimetric analyzer (TGA) (TG/DTA SII 6300 EXSTAR)
- Transmission electron microscope (TEM) (JEOL 2100 UHR-TEM)
- Tube furnace (Nabertherm, Germany)
- UV–Visible spectrometer (Lasany double-beam L1 2800)
- UV-VIS-NIR spectrophotometer (PerkinElmer, LAMBDAL6020087)
- X-ray diffractometer (XRD) (Bruker AXS D8 Advance)
- XPS (PHI 5000 Versa Probe III, Physical Electronics)

3.2 Methods

3.2.1 Preparation of CuAc/ZnAc/PAN polymeric blend solution

- Weighed 1.4g (7 Wt%) of PAN (Polyacrylonitrile) and dissolved into 10 ml of DMF (N, N-Dimethylformamide) in two glass vials.
- The as-prepared aqueous solution was magnetically stirred at 350 rpm for 30 min at room temperature.
- Weighed 700mg of copper acetate monohydrate (CuAc) and 700mg zinc acetate dihydrate (Zn Ac) and slowly dissolved them a vial. Keep mixture at magnetic stirring for 12h to get green colored solution

3.2.1 Preparation of NiAc/ZnAc/PAN polymeric blend solution

- Weighed 1.4g (7 Wt%) of PAN (Polyacrylonitrile) and dissolved into 10 ml of DMF (N, N-Dimethylformamide) in two glass vials.
- The as-prepared aqueous solution was magnetically stirred at 350 rpm for 30 min at room temperature.
- Weighed 700mg of nickel acetate (NiAc) and 700mg zinc acetate dihydrate (Zn Ac) and slowly dissolved them a vial. Keep mixture at magnetic stirring for 12h to get green colored solution.

NOTE: CuAc salt is dark green in color whereas the zinc acetate is colorless.

3.2.2 Fabrication of PAN/CuO-ZnO/NiO-ZnOnanocomposites

- Dissolved viscous solution was filled in a 3 mL syringe by keeping the distance between spinneret and collector 20cm, covered the collector with the aluminium foil
- Maintained the flowrate of solution 0.45ml/h and voltage 15kV.
- Left it for somehours,collected that nanofiber and heated at 450°C for 4 h in the presence of air to obtain CuO-ZnO and NiO-ZnOnanompositesmembrane.

3.3 Characterization

3.3.1 X- ray photoelectron spectroscopy (XPS)

Composition and electronic state studied for prepared nanocomposites evaluated by exposing the samples with X-ray beam (A1 1486 single X-ray beam) and the equipment possessing C_{10} gun with vaccum pressure of 3.75 x 10^{-14} to 3.75 x 10^{-10}torr with 20 min of time of detector acquisition. All the raw data obtained were plotted in Origin Pro 8.0 software.

3.3.2 Fourier Transform Infrared Spectrometer (FTIR) analysis

FTIR spectra of electrospun nanofibers and nanocomposites was evaluated in the range of 4000 – 400 cm^{-1} to find the functional group present in samples by Thermo Nicolet spectrometer using KBr pellets.

3.3.3Thermo Gravimetric Analysis (TGA)

Thermal stability and thermal degradation studied carried for the electro spunfiber as well as calcined pure metal oxide nanocomposites .Nearly 12mg of each sample were taken and heated in TG/DTA SII 6300 EXSTAR thermal analyzer up to temperature 800 °C with a constant heating rate of 10°C/min in presence of nitrogen atmosphere.

3.3.4 X-ray diffraction (XRD)

To determine the nature of sample whether it is crystalline or amorphous X-ray diffraction was carried out with help of Brucker AXS D8 advanced powder X-ray diffractometer with Cu-Kα radiation of wavelength λ = 1.5404Å in the range of 20° to 90° with a scan rate of 0.5°/min. Structured information were analyzed using PAN analytical xpertHighscore Plus software.

3.3.5 Field emission-scanning electron microscope (FE-SEM)

The surface morphology and size of the electro spun and calcined nanocomposites were determined by using field emission scanning electron microscope (FE-SEM) worked at 15 kV. It has energy dispersive X-ray detector (EDX) worked at an accelerating voltage of 15–20 KeV. The samples were put on twofold sided carbon tape then it is coated with gold for 80 s in Denton

gold sputtering. The samples were analyzed ImageJ software used to determine the mean diameter of the prepared samples

3.3.6 High Resolution Transmission electron microscopy (HR-TEM)

The transmission electron micrographs and selected area electron diffraction (SAED) patterns were determined by using HR-TEM operating at 200 keV with machine resolution of 0.4 nm. The sample were prepared by dissolving 1mg of sample in 2ml ethanol after that sonicated for 15min and dispersed 5ul drops onto the carbon-coated copper grids.

3.3.7 Diffuse reflectance spectroscopy (DRS)

Band gap value of metal oxide nanocomposites were calculated by getting diffuse reflectance spectra (DRS) with the help of UV-VIS-NIR spectrophotometer in the range of 250-800 nm.

3.3.8 Adsorption studies

Prepared Nanocomposites has been used for adsorption study , used 7mg of nanocomposites for the study, prepared 5 solutions of Congo red which have concentration 10ppm, 20ppm,30ppm,40ppm and 50ppm respectively.

The Langmuir adsorption isotherm equation derived from based on the assumption called monolayer assumption, another assumption there is fixed number of vacant site are available for the adsorption process and each site can hold maximum one molecule.

Linear curve between C_e/q_e versus equilibrium concentration C_e follow the Langmuir isotherm equation where K_L obtained by using slope and $q_m$obtained by using intercept of graph.

Freundlich has given the equation for the non-ideal adsorption and it is not restricted to monolayer adsorption. Freundlichconstant were obtained using slope of graph

Chapter 4 :Results and Discussion

4.1 Synthesis of nanomaterialsSynthesis of PAN/CuO-ZnOnanofibrous composites: For synthesis of PAN/CuO-ZnO/NiO-ZnO nanocomposites electrospinning technique has been used followed by heat treatment calcination. In a typical procedure, 350 mg of zinc acetate dihydrate and Nickel(ll) acetate tetrahydrate 350mg were dissolved in 5 mL of dimethylformamide separatelysame process repeated for copper acetate monohydrate solution. Thereafter, 7 wt% of PAN was added to the above solutions at room temperature. Further, zinc acetate/PAN mixture was added slowly to the copper acetate/PAN mixture under constant magnetic stirring to get a homogenous electrospinnable zinc acetate/nickel acetate/PAN(with molar ratio of Zn:Ni = 1:1) and zinc acetate/copper acetate/PAN blend polymer solution (with molar ratio of Zn:Cu = 1:1)respectively. The as-prepared viscous solution was electro spun using a 3 mL syringe, kept at a distance of 20 cm from the collector covered with aluminum foil. The flow rate of the solution was maintained at 0.45 mL/h and a fixed voltage of 15 kV between needle tip and ground collector. After few hours, a nanofibrous sheet deposited on aluminum foil which was then taken and kept for heat treatment calcination at 450°C for 4 h in the presence of air to obtainpure metal oxide NiO-ZnO and CuO-ZnO nanocomposites respectively. The complete procedure schematically represented in figure 4.1

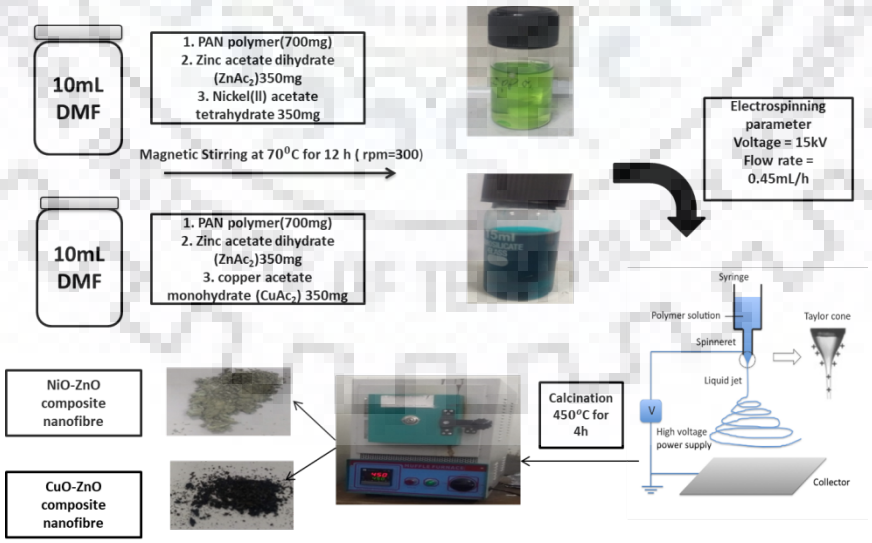

Fig 4.1: Synthesis of nanocompositefibers

4.2 FESEM (field emission scanning electron microscope)

FESEM images of electrospun $CuAc_2/ZnAc_2$/PAN $NiAc_2/ZnAc_2$/PAN nanofiber are very smooth in nature due to presence of PAN polymer. Both the electrospun nanofiber($CuAc_2/ZnAc_2$/PAN $NiAc_2/ZnAc_2$/PAN) are uniform in size it has diameter in range of nanometer.

As metal precursors solutions are not be electrospunable, some polymers needs to dissolve with metal precursor to provide template and sufficient viscosity so that it can be spin in electrospinning. After electrospinning obtained fibers heat at at 450° C for 4h, t after heating size of nanofibers decreased and surface of fiber became rough due to PAN polymer were burned.Further EDX analysis of NZ composite nanofiber has been done, where presence of Ni (30.1%), Zn (41.33%) and O (28.58%) was confirmed.

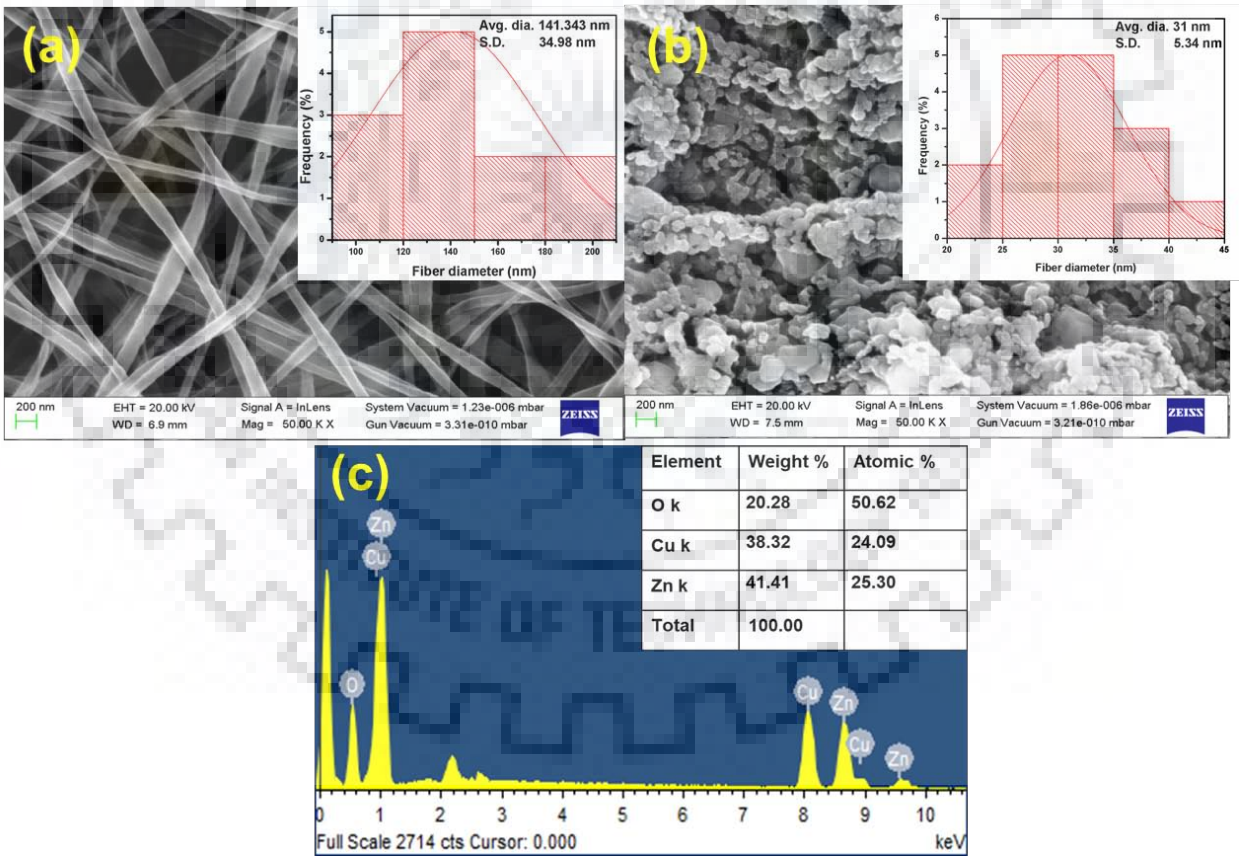

Element	Weight %	Atomic %
O k	20.28	50.62
Cu k	38.32	24.09
Zn k	41.41	25.30
Total	100.00	

Fig.4.2.1(a) Before calcination (b) After calcination (c) EDX of calcined CZ composite nanofiber

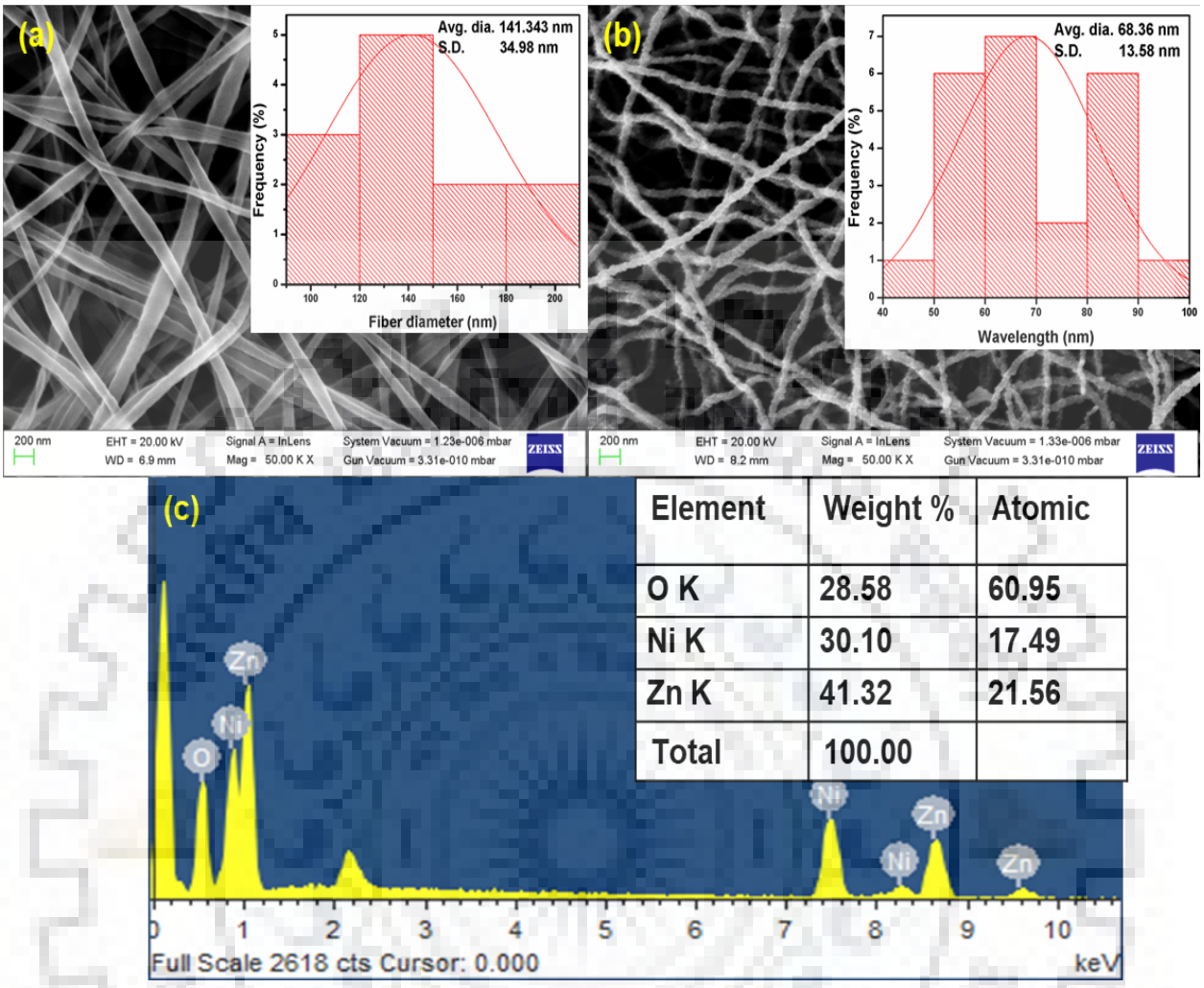

Fig 4.2.2.(a) Before calcination (b) After calcination (c) EDX of calcined NZ composite nanofiber

4.3 High Resolution –Transmission electron microscopy (HR-TEM) analysis

Figure shows that nanocomposite synthesized by the electrospinning after that calcination technique. Figure (a) shows the nanofiber having the size 67.51nm for NZ nanocomposite , figure (b) , it shows the selected area electron diffraction (SAED) pattern of NZ nanocomposite, continues bright ring defined to crystalline nature of NZ nanocomposite, whereas for CZ nanocomposite cluster of CZ is found in the range of 30nm to 41nm.

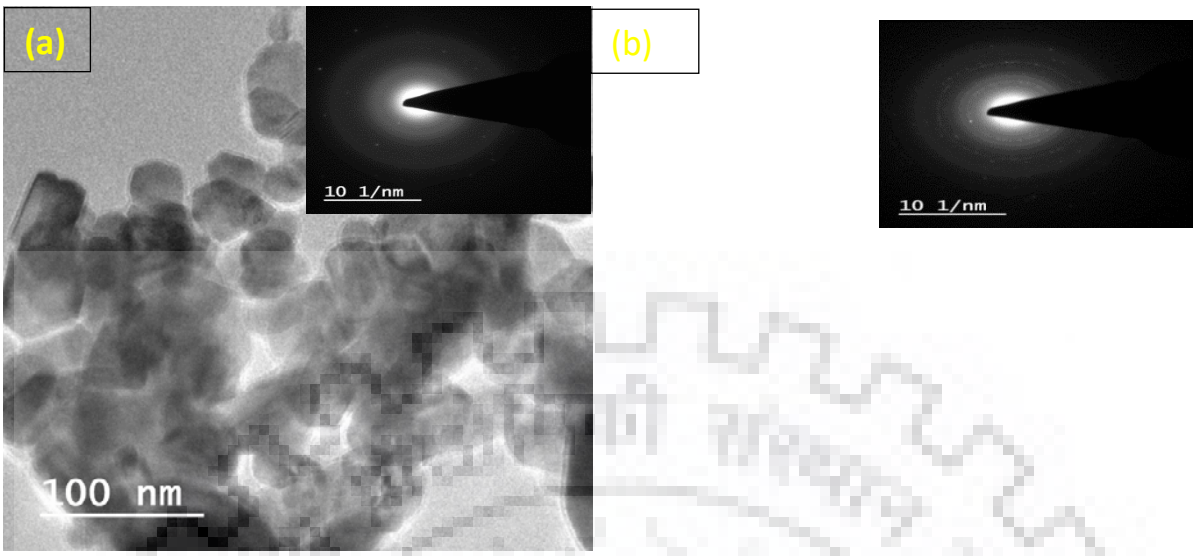

Fig: 4.3 TEM image of (a) CZ and (b) NZ composite nanofibers with their respective SAED pattern

4.4X-ray Diffraction (XRD)

To analyzed the crystalline and amorphous nature of prepared nanofibers powder X-ray diffraction (XRD) instrument has been used further acquired data evaluated by PANalyticalX'pert High Score Plus software. Figure 4.2(a) representsPrepared electrospun $CuAc_2/ZnAc_2$/PAN $NiAc_2/ZnAc_2$/PAN nanofiber showing broad peaks broad peaks found between 22.5º and 35° which demonstrate the amorphous nature of fiber due to presence of PAN polymer the typical XRD pattern of electrospun fiber of where standard peaks of all metal oxides formed are observed. The characteristic diffraction peaks indexed to 2θ are 47.55°,56.22°, 62.19° and 67.58° could be indexed to (102), (110), (103) and (112) crystal planes respectively which is showing the hexagonal nature of ZnO with reference to JCPDS card number 01-079-0208. intense peaks appeared at 38.48 and 65.85° corresponding to (111), (022) which indicates monoclinic phase of (JCPDS no 00-048-1548).The index at 2θ = 36.49° correspond to (111) shows cubic nature of Cu_2O(JCPDS no 00-003-0892).Apart from this ,intense peaks at 43.40°,63.02°,75.51°,79.52° could be indexed to (200), (220), (311) and (222) which correspond to (JCPD no 01-073-1519) indicate cubic nature of NiO.The crystallite size of metal oxide nanofibrous membrane was also determined using the Debye Scherrer formula: $t = K\lambda / B\cos\theta$, where t is the crystallite size , K is numeric constant of value 0.9 , λ is wavelength of Cu Kα

radiation which is equal to 0.154 nm , B is full width at half maximum (FWHM). Using this above formula, the size of metal oxide nanofibrous membrane was found to be less than 10 nm.

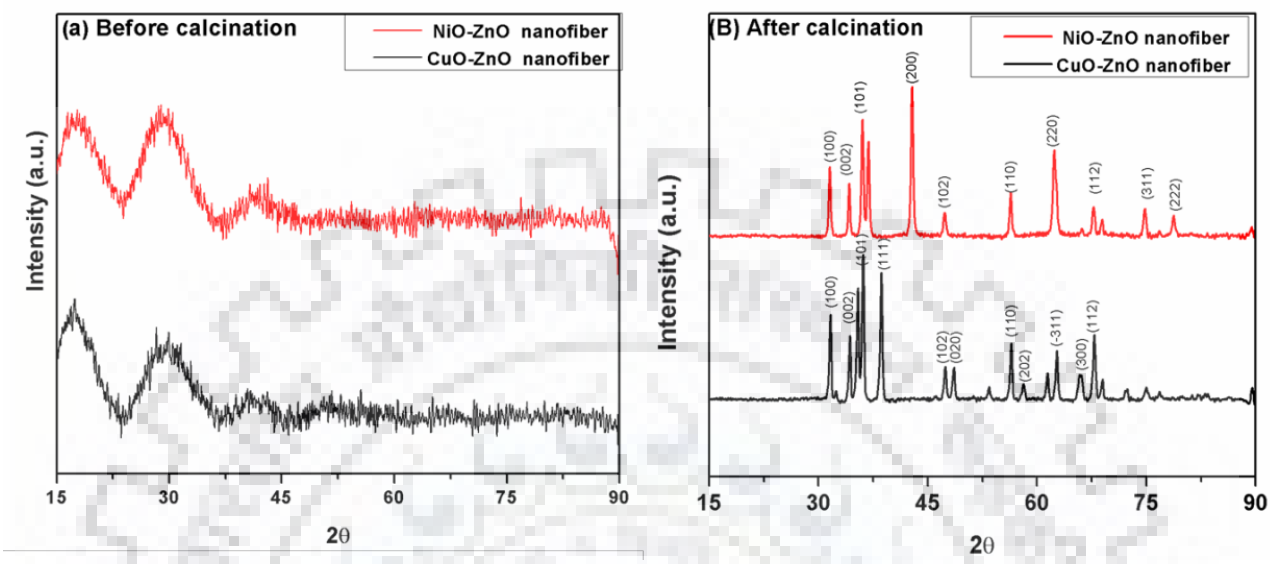

Fig 4.4:XRD pattern for NZ and CZ (a) Before calcination and (b) After calcination

Sample name	Angle (2θ)	Crystal plane	JCPDS no	Crystal structure
ZnO	47.35 56.22 62.19 67.58	(102) (110) (103) (112)	01-079-0208	Hexagonal
CuO	38.48 65.85	(111) (022)	00-048-1548	Monoclinic
Cu_2O	N.A	N.A	00-002-1067	Cubic
NiO	37.34 43.40 63.02 75.51 79.52	(111) (200) (220) (311) (222)	01-073-1519	Cubic

Table4.4 XRD data of NZ and CZ composite nanofiber

4.5 Fourier Transform Infrared (FTIR) analysis

Function group of prepared metal oxide CuO-ZnO and NiO-ZnO nanocomposites were obtained by Fourier Transform Infrared (FTIR) spectrum analysis.A peak at 3400 cm^{-1}indicates presences of –OH functional group over the surface of NiO-ZnO and CuO-ZnO.(Ashok et al., 2016)Additional peaks from 1622 cm^{-1} to 1326 cm^{-1} ascribed to stretching vibrations of –CH group both in hydrothermal and calcined sample. A sharp peak at 1383.13 cm^{-1}indicates presence of symmetry vibration of COO^{-} in metal oxidesThe 479.8 cm^{-1}allocated for metal oxygen (M-O) stretching bond.(Mansur et al., 2008)

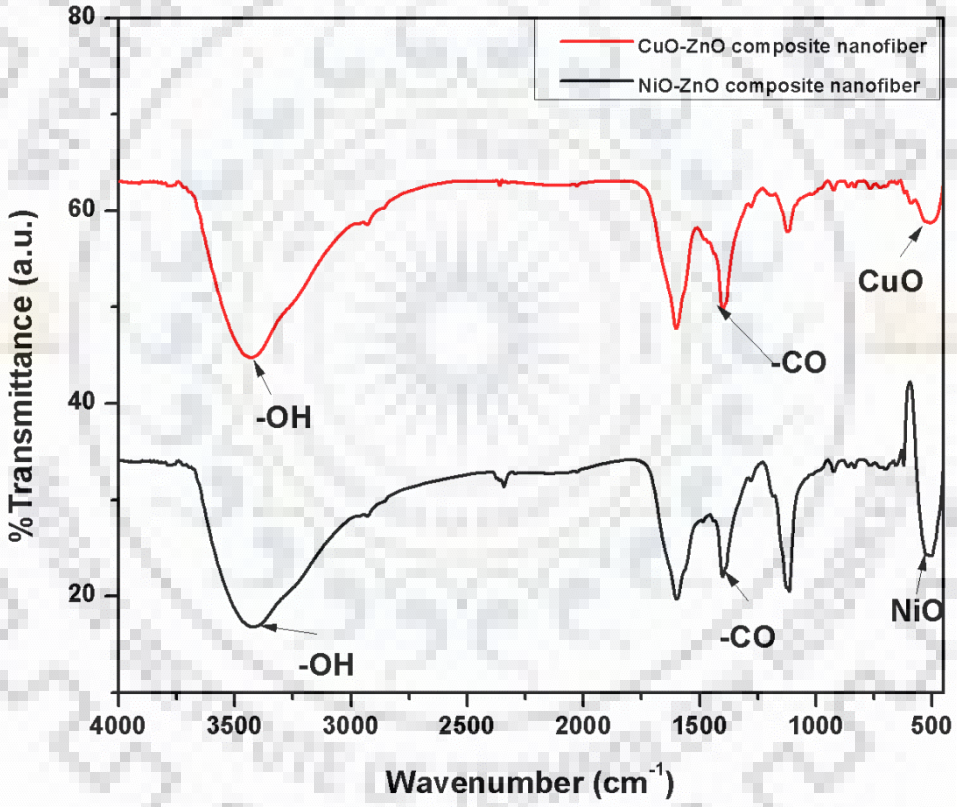

Fig:4.5 FTIR image of NZ and CZ nanofiber

4.6Thermo Gravimetric analysis

How the chemical decomposition behavior of electrospun nanofiber and calicinednanofiber(nanocomposites) vary with time was investigated using the thermogravimetric analysis (TGA). The nanofibrous membranes follow the uniform degradation profile after hydrothermal treatment.The initial weight loss occurred for CuAc-$ZnAc_2$ till 200 ºC and for NiAc-$ZnAc_2$ till 220 °C because of absorption of moisture and low molecular weight solvents present electrospun nanofiber. Thereafter in range it undergo cleavage of C-C bonding in polyacrylonitrile (PAN) polymer200 °C to 280 °C and 230 °C to 330 °Cfor CuAc-$ZnAc_2$and NiAc-$ZnAc_2$respectively. Further it go carbon combustion which cause to loss nearly 80% weight loss. At the end of 800°C 24.4% and 19.5% by weight loss for CuAc-$ZnAc_2$and NiAc-$ZnAc_2$respectively. which confirms the thermal stability of CuO-ZnOnanofibrous membrane whereas, In calcination 99% by weight residues left for both pure metal oxides nanocoposites(NiO-ZnO, CuO-ZnO),this is because after calcination there were no polymer(PAN) present in the sample as a result we have obtained pure metal oxides which is thermally stable as comparative to electrospun. Moreover, in calcination process there is initial loss of weight could be due to the moisture and unreacted component.

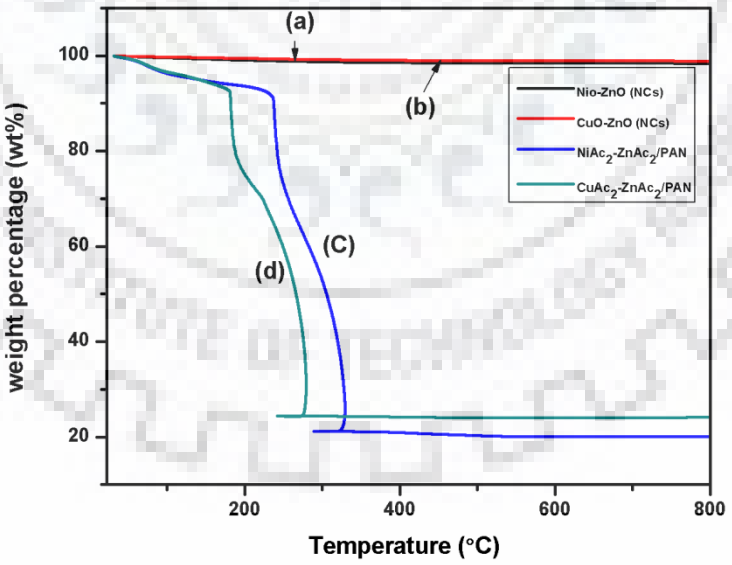

Fig4.6 : TGA curve (a),(b) before calcination and (c) and after calcination for NZ and CZ composite nanofibers

4.7 Diffuse Reflectance Spectroscopy (DRS) analysis

For the calculation of energy band gap of NZ and CZ nanocomposites, diffuse reflectance spectroscopy (DRS) has been performed. Since prepared nanocomposites have been used for photocatalytic reaction. , we need to find out if synthesized nanocomposites are semiconductors, thus band gap value is evaluated ((Khorrami et al., 2015).

Kubelka and Munk have developed the equation to find out the diffuse reflectance analysis of inhomogenous materials("What is Kubelka-Munk ?," n.d.).

$$F(R) = (1- R)^2 / 2R$$

Where, F(R) denoted the Kubelka-Munk (K-M) function and R indicates absolute reflectance. The band gap energy of CZ and NZ evaluted by the following equations

$$F(R) \times h\nu = A(h\nu - Eg)^n$$

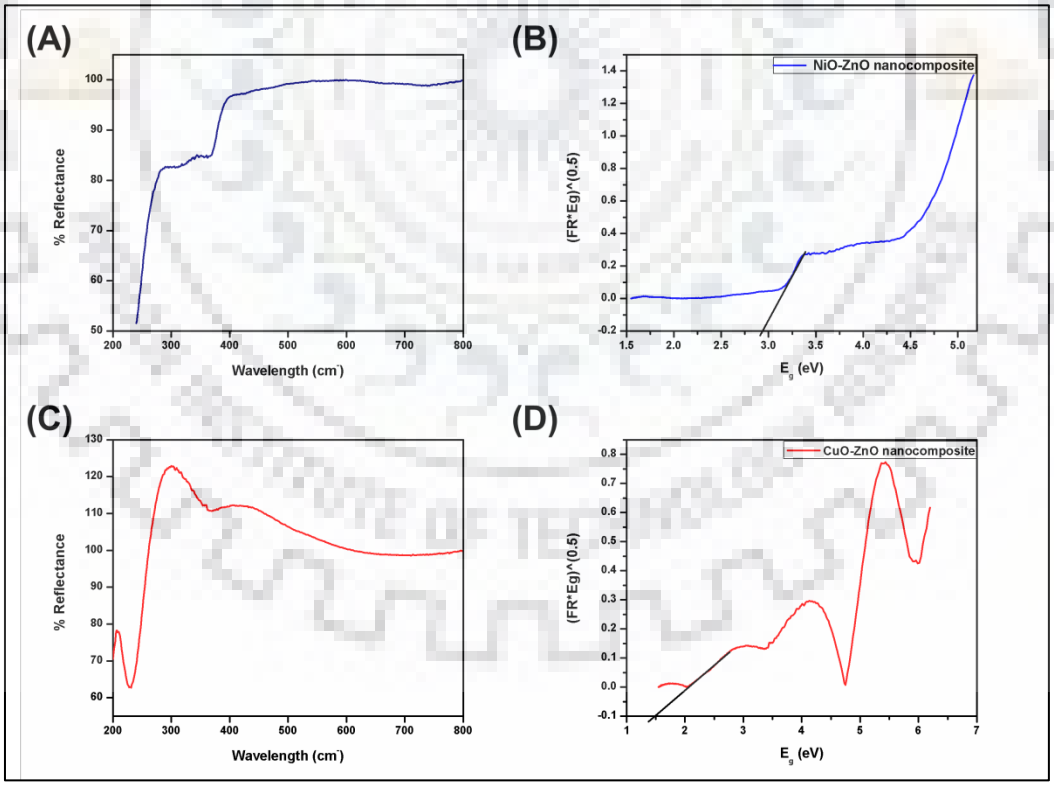

Fig 4.7 (A),(C) Diffuse reflectance spectra, (B) and (D) optical band gap of NZ and CZ composite nanofibers,

Where, hv denotes the energy band gap , Eg band gap energy where as A represent and proportionality constant. In addition to, n denotes the mode of electronic transition in the semiconductor i.e. n = ½, for direct shift of electron and n = 2, for indirect shift. From the plots of $[F(R) \times h\nu]^{1/2}$ Vs hν, the band gap values have been calculated. The estimated band gap is 1.51 eV and 2.95 eV for CuO-ZnO and NiO-ZnO, respectively. Thus, it clearly reveals the formation of p-n heterojunction between CuO and ZnO.

4.8 Photocatalytic Studies

Comparative study between NZ and CZ composite nanofibers

4.8.1In presence of sunlight

For the dye degradation study in presence of sunlight, prepared 20ppm concentration of congo red and taken 4,7,10mg different concentration of photocatalyst(NZ and CZ). It was observed both the photocatalyst(NZ and CZ) were taking similar time to degrade the Congo red dye.:

To investigate the better photocatalyst, the efficiencies of both samples(NZ,CZ) were compared. The photocatalytic activity of the samples was examined by the degradation of CR dye in the presence of sunlight.it was found that time taken to for the removal of dye achieved same in both the case solution containing NZ and CZ, ,both the fiber were showing similar dye removal efficiency.

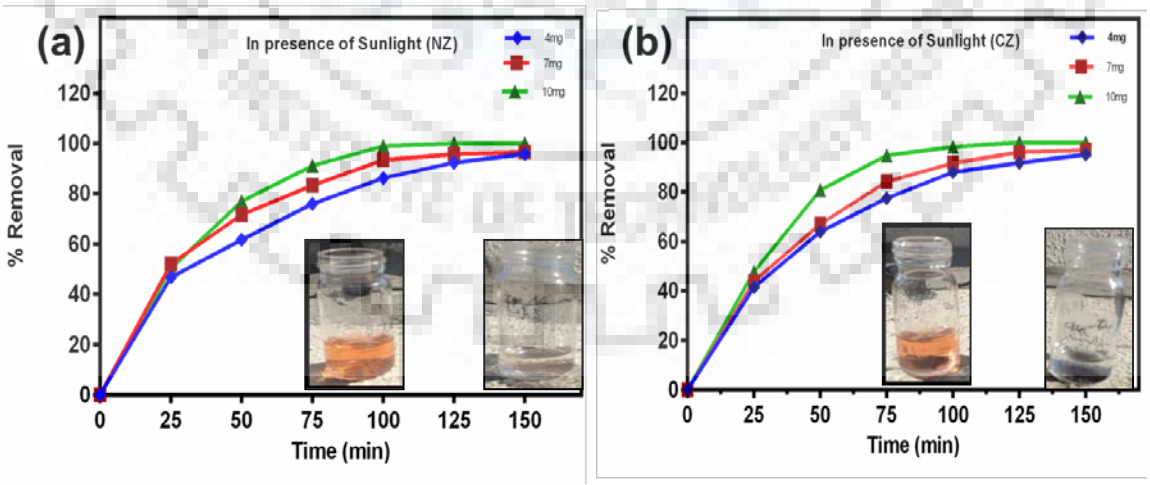

Fig: 4.8.1 Photodegadation of dye (a) with NZ and (b) with CZ

Kinteic study

Kinetic study was done and rate constant value has been calculated for the photocatalytic reaction. the graph has been plottedbetween $\ln(C_0/C_t)$ and time (min) where C_0denotes the intial concentration and $C_t$is instant concentration of dye. The data has been plotted between $\ln(C_0/C_t)$ and time

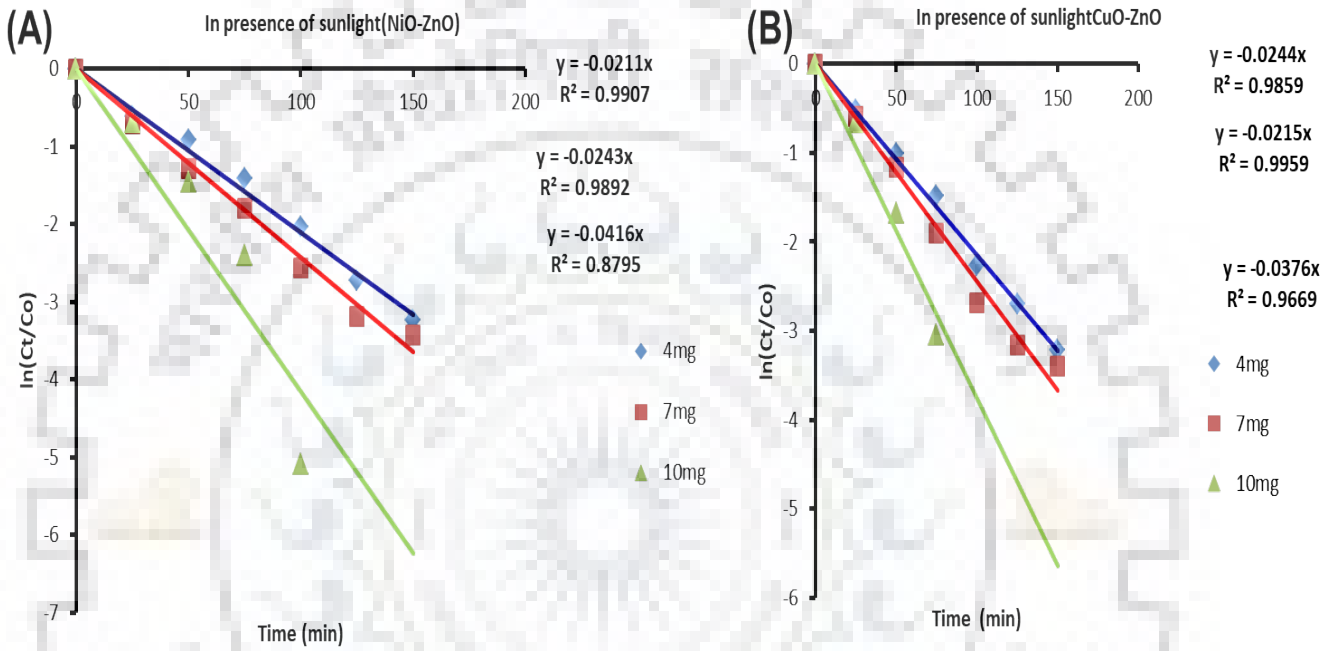

Fig 4.1.2 Dye removal kinetics study in presence of Sunlight (iii) with NZ and (iv) with CZ nanocomposite fiber

Sample	Rate constant,k(per minute)	Rate constant, k (per minute)	Rate constant,k(per minute)
Catalyst	**4mg**	**7mg**	**10mg**
NiO-ZnO	**0.0211**	**0.0243**	**0.0416**
CuO-ZnO	**0.0215**	**0.0244**	**0.0376**

Table 4.8.1 Rate constant of NZ and CZ composite nanofibers

4.8.2 In absence of sunlight with shaking:

Adsorption efficiency of CZ and NZ nanocomposites was examined with congo red dye solution. UV-visible spectrum showed the gradully reduction of congo red with time. Prepred 20ppm of dye (Congo red) solution , and used 4,7,10mg of nanocomposites The concentation of dye calculated at interval of 25 minutes. In figure it is clearly showing when 10 mg NZ used , it was found 84% of dye removed, whereas only 50% of dye removed in case of CZ while maintaining the same parameter. Nearly 99% dye removal achived in just 175 minutes in case of NZ, wheras CZ were taking 225 minutes to remove the same.

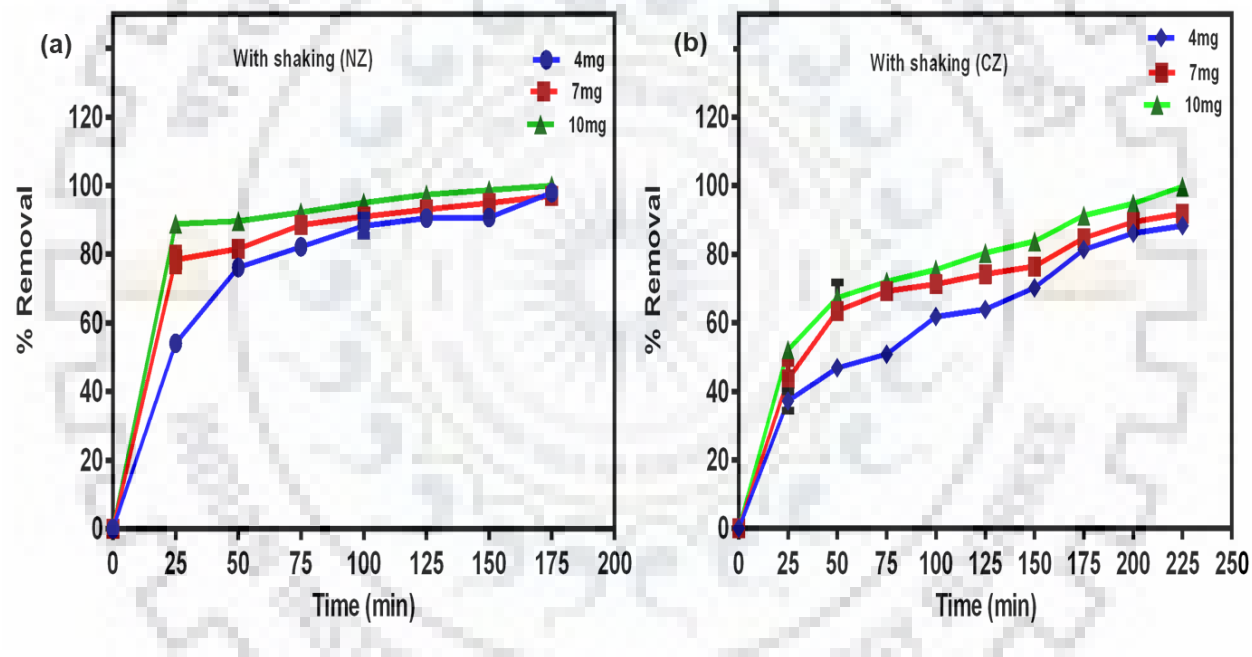

Fig4.8.2 Dye removal kinetics study in presence of Sunlight (A) with NZ and (B) with CZ nanocomposite fiber

4.8.3 In absence of sunlight without shaking

In case of absence of sunlight without shaking, It was observed that NZ were showing better adsorption efficiency than CZ for removing the nearly 99% dye from the solution. NZ is taking 225 min, while CZ is taking 250 min for same.

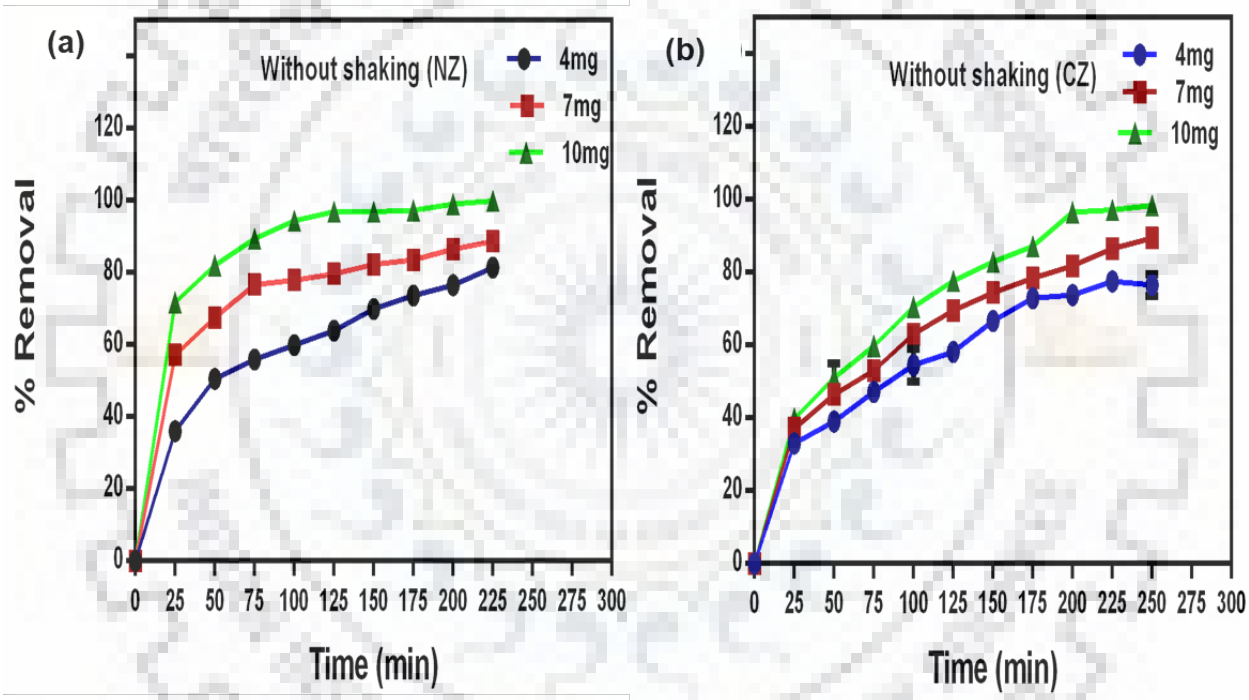

Fig 4.8.3 Dye removal kinetics study in presence of Sunlight (A) with NZ and (B) with CZ nanocomposite fiber

4.9 X-Ray photoelectron spectroscopy (XPS)

CZ

XPS is an excellent technique to determine the structure and compositions of element present in the sample,after adsorption process CZ nanocomposite fiber were analyzed whether congo red's element present on the adsorbentsurface, so for verifying the adsorption process XPS of adsorbent CZ nanocomposites fiber was performed, figure 4.9.1 is represent the presence of element and their oxidation state respectively.

The characteristicspeak obtained at 1021.8 eV and 1045eV assigned for $Zn2P_{3/2}$ and $Zn2P_{1/2}$ respectively. The broad peak at 530.31 eV is attributed to O1s.the peak at 933.2 eV and 952.94 eV is located for $Cu2P_{3/2}$ and $Cu2P_{1/2}$ respectively. The XPS spectra reveals binding energy of carbon at about 285.8 eV, it represent the C-C bon

NZ

In Fig 4.9.2 (a), (b), (c), (d), (e) and (f) represent the represent the overall spectrum of NZ and the elements presence with their respective oxidation state t in the adsorbent after the adsorption of Congo red, it indicates the presence of N,C,O,Zn and nickel. The peak found at 285 eV is attributed to $C1_s$ (C-C and C-H bonds), the broad and asymmetric peak of O1s indicates the presence of multicomponent species. it can resolve by using the curve fitting method, first one attributed at 530 eV and second one attributed at 532.4. the characteristics peak obtained at 1021.8 eV and 1045eV assigned for $Zn2P_{3/2}$ and $Zn2P_{1/2}$ respectively. The peak obtained at 857.5 eV is assigned for the $Ni2p_{3/2}$(Khaleed et al., 2017).

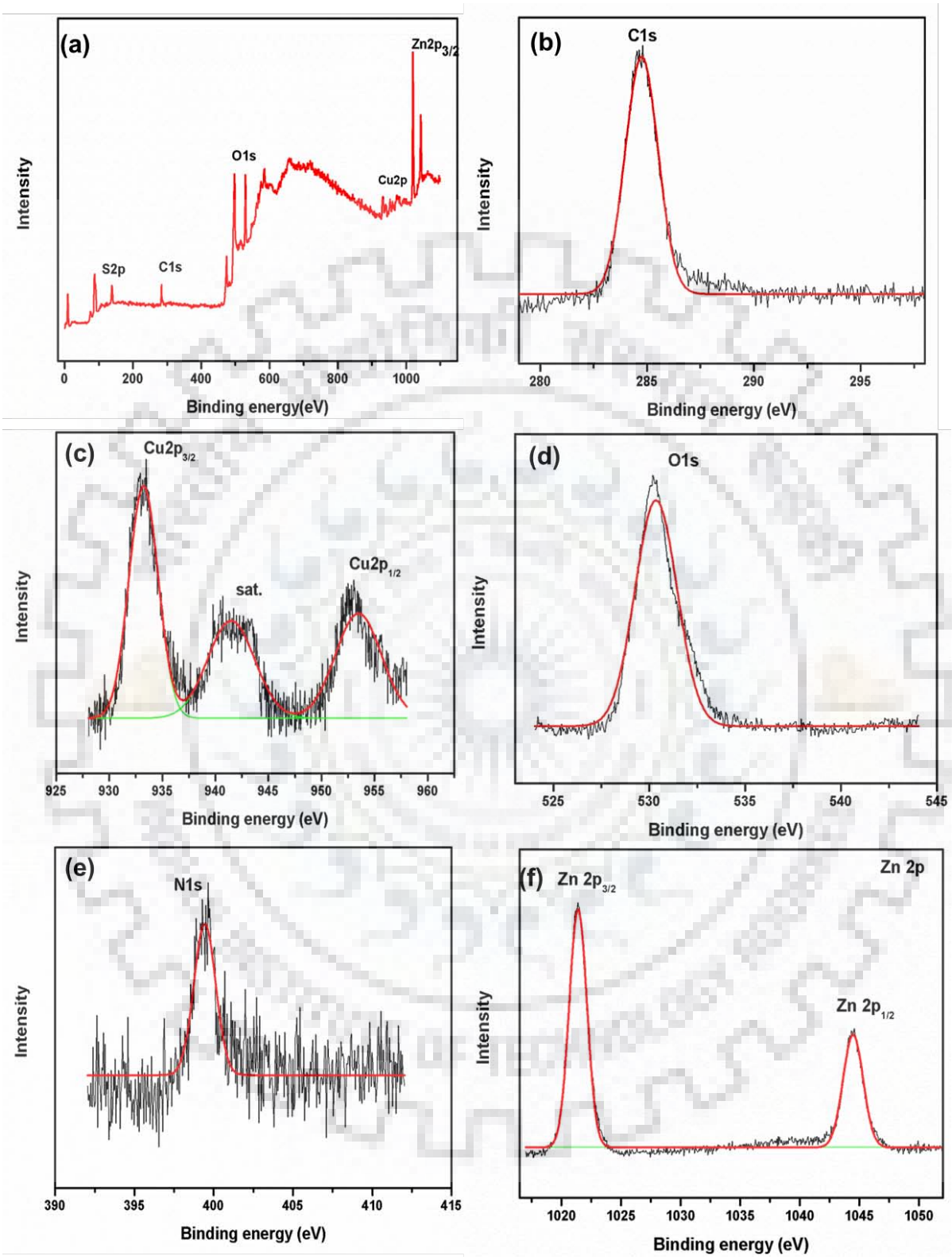

Fig4.9.1 XPS data of CZ composite nanofiber after adsorption

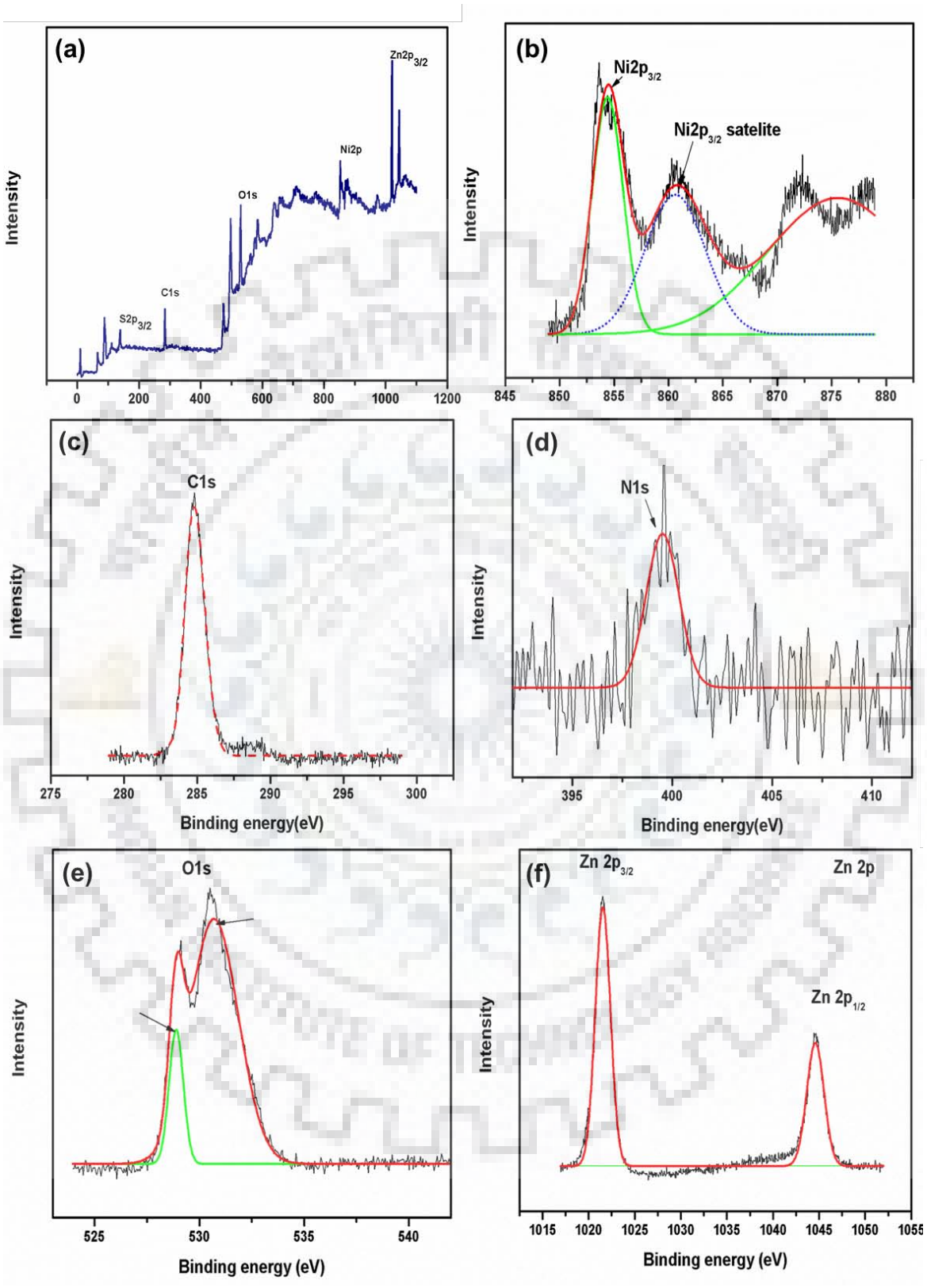

Fig 4.9.2 XPS data of NZ composite nanofiber after adsorption

4.10 Isothermal study

The adsorption kinetics of NZ and CZ composite nanofiber were fitted by two models Langmuir and freundlich

$$\frac{C_e}{q_t} = \frac{C_e}{q_m} + \frac{1}{kq_m}$$

$$\ln q_e = \ln K_f + \frac{1}{n} \ln C_e$$

where q_t is the adsorption amount at time t, Ce is the equilibrium concentration and q_m is the maximum adsorption capacity k and K_f are the Langmuir and frenudlich adsorption proportionality constant . 1/n is the hetrogenous factor (Patiha et al., 2016).

for the experimental data high co-reltion value obtained for the freundlich model and it suggest that our adsorption is non ideal(Liu et al., 2015)

Experimental result was examined using two empirical equation Langmuir and freundlichThe Langmuir adsorption isotherm equation derived from based on the assumption called monolayer assumption, another assumption there is fixed number of vacant site are available for the adsorption process and each site can hold maximum one molecule.

Linear curve between C_e/q_e versus equilibrium concentratin $C_e$follow the Langmuir isotherm equation where K_L obtained by using slope and $q_m$obtained by using intercept of graph.

Freundlich has given the equation for the non ideal adsorption and it is not restricted to monolayer adsorption . freundlich constant were obtained using slope of graph

And n were calculated by using intercept of the graph.

4.10.1 Longmuir isotherm

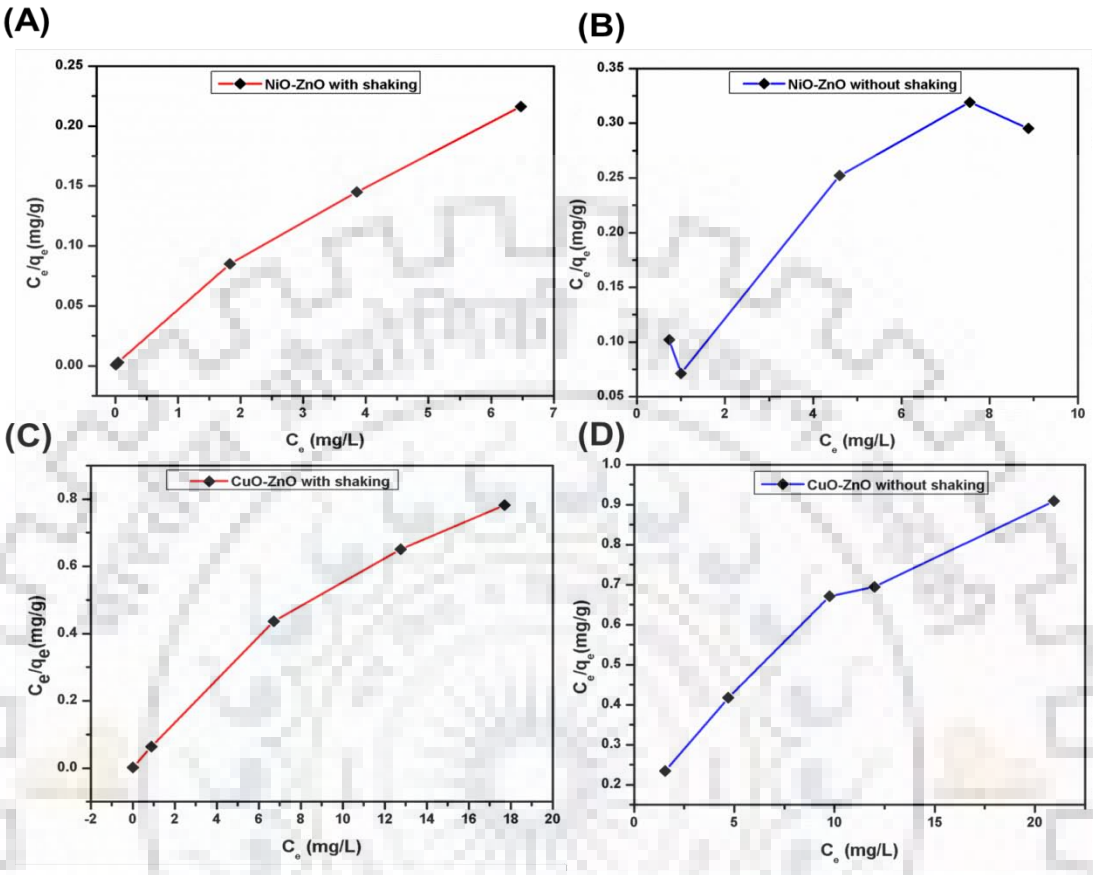

Fig 4.10.1 Langmuir Isother curve (A) , (B) with and without shaking (NZ) and (C), (D) with and without shaking for (CZ)

Sample	NZ		CZ	
Parameters	With shaking	Without shaking	With shaking	Without shaking
R^2	0.98164	0.87006	0.9584	0.918
q_m	29.9401	34.3643	29.9401	33.34
K_L	4	0.3875	0.9565	0.12

Table 4.10.1 Parameter Langmuir Isotherm (A) , (B) with and without shaking (NZ) and (C), (D) with and without shaking for (CZ)

From the table it can clearly see in caseof NZnanocomposite without shaking , maximum value of q_m(maximum adsorption capacity) is 34.3643 mg/g for Langmuir isotherm.

4.10.2 Freundlich Isotherm

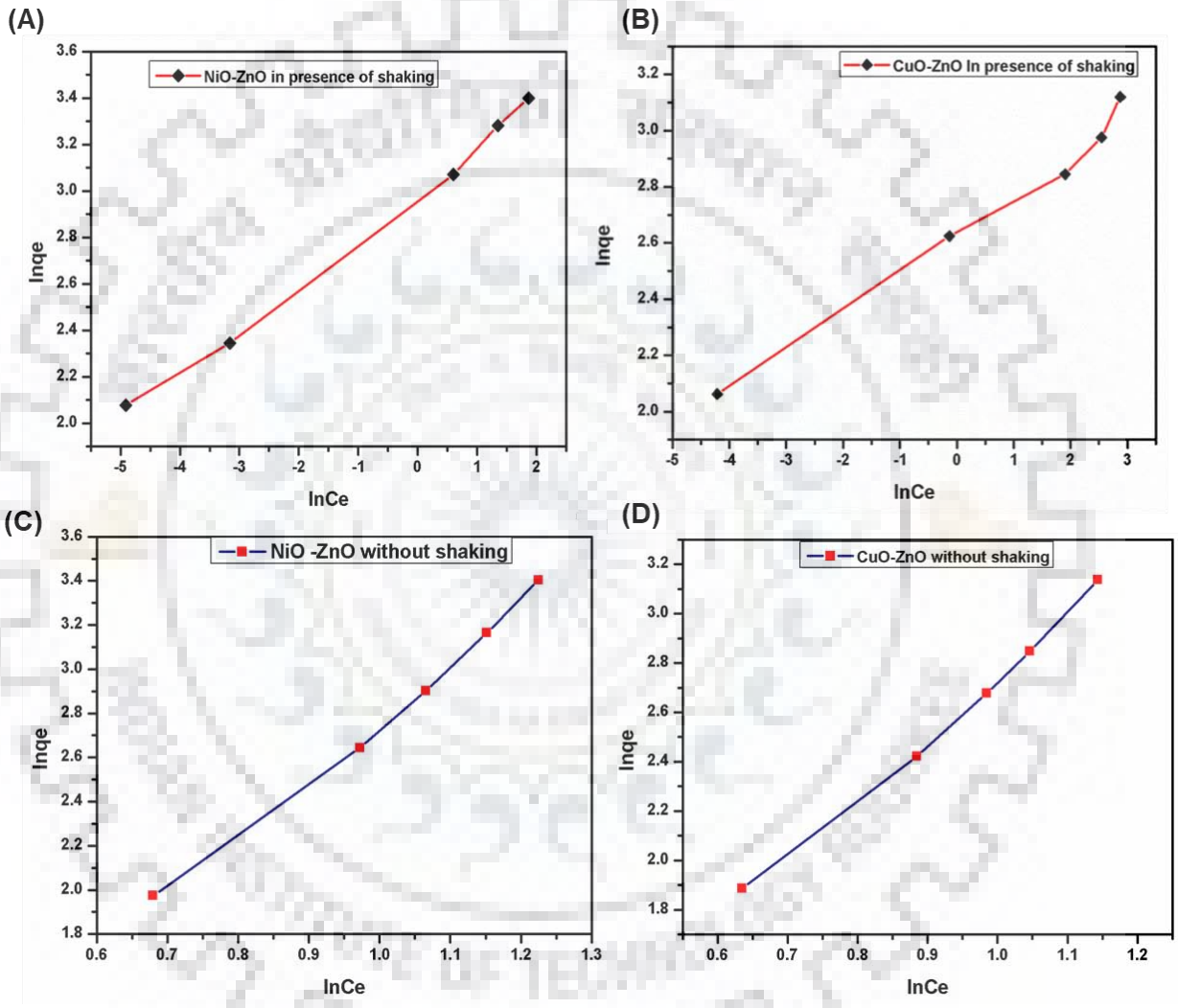

Fig 4.10.2 FreundlichIsotherm curve (A) , (B) with and without shaking (NZ) and (C), (D) with and without shaking for (CZ)

From the co relation (R^2) value It was found the data fit to freundlich adsorption in all of the cases. Maximum value of $K_F$was found 20.0855 mg/g in case of with shaking for NZ.

4.11 Kinetic study

Adsorption mechanism can be explain by , dye molecule adsorbed or stick on the surface of adsorbent then it starts moving inside the pores of adsorbent and start occupy the active site/empty space of adsorbent; once actives filled the rate of diffusion decrease and hence the adsorption become slow or stop(Pan et al., 2017). To study the rate of adsorption kinetic, kinetics

$$\ln(q_e - q_t) = \ln q_e - kt \quad \text{..... (1)}$$

$$\frac{t}{q_t} = \frac{1}{k_2 q_e^2} + \frac{t}{q_t} \quad \text{.....(2)}$$

equaition (1) reperenst the first order psuedo kinetics plot and and eqution (2) represent the second order psuedo kinetics, where as q_e is the equlibrium adsorption capacity (mg/g), k and k_2 is first and second order rate constant respectively. For pseudo first order plot and it is a plot of $\ln (q_e - q_t)$ vs t and for pseudo second order it is a plot of t/q_t vs t.

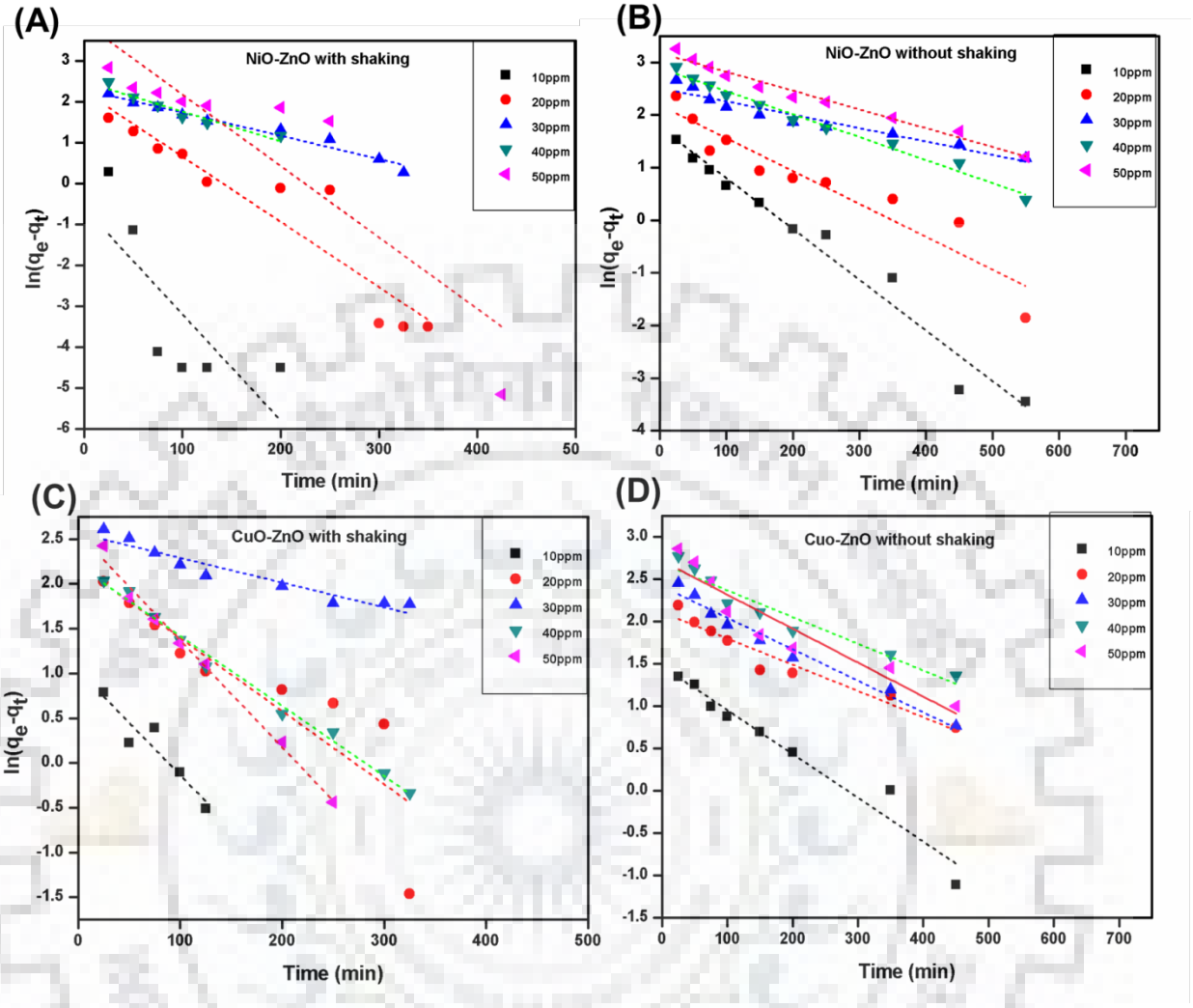

Fig 4.11.1 Pseudo first order kinetic plot (a) ,(b) with and without shaking (NZ), (c) and (d) with and without shaking (CZ)

(a) NZ with shaking

Concentration (ppm)	10	20	30	40	50
Slope (k)	0.0260	0.0159	0.0056	0.0072	0.0174
q_e (mg/g)	0.55	9.5611	10.00442	12.1024	50.4968
R^2	0.4876	0.8656	0.96295	0.9074	0.7578

(b) CZ with shaking

Concentration(ppm)	10	20	30	40	50
Slope (k)	0.01168	0.00817	0.0276	0.00782	0.01195
q_e (mg/g)	2.8116	9.1321	13.0203	9.0291	13.1638
R^2	0.8392	0.74864	0.90956	0.98976	0.98975

(c) NZ without shaking

Concentration (ppm)	10	20	30	40	50
Slope (k)	0.009	0.006	0.002	0.004	0.003
q_e (mg/g)	5.8206	8.8809	12.3259	17.9969	23.955
R^2	0.90644	0.8860	0.9242	0.982	0.975

(d) CZ without shaking

Concentration (ppm)	10	20	30	40	50
Slope (k)	0.00510	0.00309	0.00372	0.00315	0.00401
q_e (mg/g)	4.3562	8.2391	11.1960	14.6402	15.0577
R^2	0.94854	0.93143	0.9718	0.92467	0.8824

Table4.11.1 Represent the kinetics parameters of pseudo first order kinetic plot (a) ,(b) with and without shaking (NZ), (c) and (d) with and without shaking (CZ)

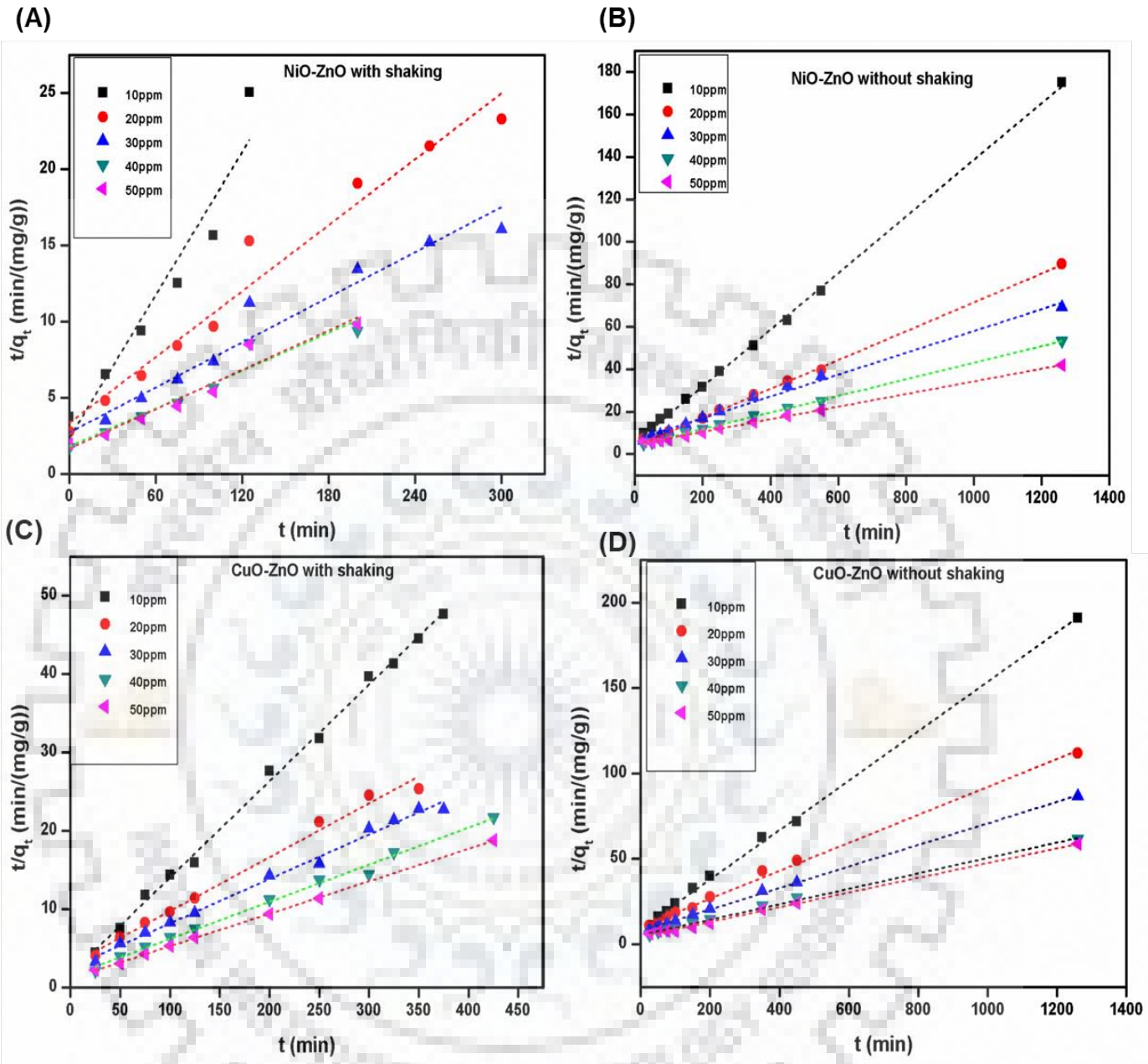

Fig 4.11.2 Pseudo second order kinetic plot (a) ,(b) with and without shaking (NZ), (c) and (d) with and without shaking (CZ)

(a) NZ with shaking

Concentration (ppm)	10	20	30	40	50
K_2 (g/mg/min)	0.010395	0.001555	0.000893	0.000951	0.00117
q_e (mg/g)	6.3881	13.8658	20.2716	24.1371	23.2342
R^2	0.91171	0.96374	0.9514	0.92376	0.93278

(b) NZ without shaking

Concentration (ppm)	10	20	30	40	50
K_2 (g/mg/min)	0.003317	0.001298	0.000398	0.000384	0.000199
q_e (mg/g)	7.5586	14.7275	19.4932	25.6441	33.67
R^2	0.99997	0.9983	0.99135	0.9994	0.9981

(c) CZ with shaking

Concentration (ppm)	10	20	30	40	50
K_2 (g/mg/min)	0.008939	0.001643	0.001277	0.001543	0.001539
q_e (mg/g)	8.1235	14.556	17.6678	21.1416	24.1546
R^2	0.99731	0.9886	0.99252	0.993	0.9997

(d) CZ without shaking

Concentration (ppm)	10	20	30	40	50
K_2 (g/mg/min)	0.00232	0.064804	0.000512	0.000381	0.000418
q_e (mg/g)	6.9118	1.1226	15.8604	22.1435	23.218
R^2	0.99845	0.99587	0.9987	0.99691	0.9974

Table4.11.2 Represent the kinetics parameters of pseudo second order kinetic plot (a) ,(b) with and without shaking (NZ), (c) and (d) with and without shaking (CZ)

From the co relation (R^2), it was observed experimental data are following the second order pseudo kinetics in NZ as well CZ composites nanofibers all the condition (with shaking and without shaking) , maximum value of q_e is 33.67 mg/g in 50 ppm concentration (NZ without shaking) and K_2 = 0.01095 g/mg/min in 10 ppm (NZ with shaking)

CHAPTER 5 CONCLUSION

In summary, we have successfully fabricatedNiO-ZnO(NZ) andCuO-ZnO(CZ)nanofibrous composites using simple electrospinning technique followed by post heat treatment methods calcination. The synthesized nanofibrous materials were characterized by several analytical techniqiues. The comprehensive batch wise dye degradation and kinetic studies supplemented the effective photocatalytic activity of the synthesized nanomaterials. It was observed that in photocatalytic degradation(presence of sunlight) NZ and CZ composite nanofibers were showing the similar removal efficiency where as In adsorption NZ composite nanofiber were showing much better result than CZcomposite nanofiber. So we can conclude for indoor application we can use NZ and for outdoor if sunlight presents in sufficient amount we can use CZ nanofiber composite.

Future scope

for outdoor application pilot scale photocatalytic reactor can be build, where NZ or CZ can be used for the degradation of dyes and others pollutant, as our studies proved in presence of sunlight NZ and CZ composite nanofiber were removing the dye at same rate .synthetic nanofibrous membrane to be placed at the bottom and the industrial dyes and pollutant containing toxic chromophore agent undergo degradation through photcatalysis under solar irradiation

After comprehensive analysis and experiments, a laboratory based photocatalytic reactor needs to be developed in which the synthetic polymeric nanofibrous membrane to be placed at the bottom and the industrial dye pollutants containing toxic chromophore agents undergo degradation through photocatalysis under solar irradiation followed by collection of treated water through the outlets and the same idea can be scaled up as per industrial requirements

CHAPTER 6 REFERENCES

1) Afkhami, A., Moosavi, R., 2010. Adsorptive removal of Congo red, a carcinogenic textile dye, from aqueous solutions by maghemite nanoparticles. J. Hazard. Mater. 174, 398–403. https://doi.org/10.1016/j.jhazmat.2009.09.066
2) Ashok, C., Rao, K.V., Chakra, C.S., 2016. Facile synthesis and characterization of ZnO/CuO nanocomposite for humidity sensor application. Chem. Sci. J. Adv. Chem. Sci. 2, 223–226. https://doi.org/10.5185/amp.2016/111
3) Bandekar, G., Rajurkar, N.S., Mulla, I.S., Mulik, U.P., Amalnerkar, D.P., Adhyapak, P. V., 2014. Synthesis, characterization and photocatalytic activity of PVP stabilized ZnO and modified ZnO nanostructures. Appl. Nanosci. 4, 199–208. https://doi.org/10.1007/s13204-012-0189-2
4) Choksumlitpol, P., Mangkornkarn, C., Sumtong, P., Onlaor, K., Eiad-Ua, A., 2017. Fabrication of Anodic Titanium Oxide (ATO) for waste water treatment application. Mater. Today Proc. 4, 6124–6128. https://doi.org/10.1016/j.matpr.2017.06.104
5) Dhineshbabu, N.R., Vetumperumal, V.R.N.N.R., 2016. Study of structural and optical properties of cupric oxide nanoparticles. Appl. Nanosci. 6, 933–939. https://doi.org/10.1007/s13204-015-0499-2
6) El-Kemary, M., Nagy, N., El-Mehasseb, I., 2013. Nickel oxide nanoparticles: Synthesis and spectral studies of interactions with glucose. Mater. Sci. Semicond. Process. 16, 1747–1752. https://doi.org/10.1016/j.mssp.2013.05.018
7) Gao, F., Peng, Z., Fu, X., 2013. One-Step Synthesis and Characterization of Silica Nano-/Submicron Spheres by Catalyst-Assisted Pyrolysis of a Preceramic Polymer. J. Nanomater. 2013, 1–4. https://doi.org/10.1155/2013/843570
8) Gao, S.J., Shi, Z., Zhang, W. Bin, Zhang, F., Jin, J., 2014. Photoinduced superwetting single-walled carbon nanotube/TiO 2 ultrathin network films for ultrafast separation of oil-in-water emulsions. ACS Nano 8, 6344–6352. https://doi.org/10.1021/nn501851a
9) Gogoi, S.K., Gopinath, P., Paul, A., Ramesh, A., Ghosh, S.S., Chattopadhyay, A., 2006. Green fluorescent protein-expressing Escherichia coli as a model system for investigating the antimicrobial activities of silver nanoparticles. Langmuir 22, 9322–9328. https://doi.org/10.1021/la060661v

10) Grandgirard, J., Poinsot, D., Krespi, L., Nénon, J.P., Cortesero, A.M., 2002. Costs of secondary parasitism in the facultative hyperparasitoid Pachycrepoideus dubius: Does host size matter? Entomol. Exp. Appl. 103, 239–248. https://doi.org/10.1023/A
11) Huang, Z.M., Zhang, Y.Z., Kotaki, M., Ramakrishna, S., 2003. A review on polymer nanofibers by electrospinning and their applications in nanocomposites. Compos. Sci. Technol. 63, 2223–2253. https://doi.org/10.1016/S0266-3538(03)00178-7
12) Indexed, S., Nadu, T., Chellaiah, G., Nadu, T., Selvakumar, P.M., Nadu, T., 2018. A REVIEW OF NANO PARTICLE APPLICATION 9, 381–387.
13) Janotti, A., Walle, C.G. Van De, 2009. Fundamentals of zinc oxide as a semiconductor 72. https://doi.org/10.1088/0034-4885/72/12/126501
14) Khaleed, A.A., Bello, A., Dangbegnon, J.K., Madito, M.J., Olaniyan, O., Barzegar, F., Makgopa, K., Oyedotun, K.O., Mwakikunga, B.W., Ray, S.C., Manyala, N., 2017. Solvothermal synthesis of surfactant free spherical nickel hydroxide / graphene oxide composite for supercapacitor application Solvothermal synthesis of surfactant free spherical nickel hydroxide / graphene oxide composite for supercapacitor application. J. Alloys Compd. 721, 80–91. https://doi.org/10.1016/j.jallcom.2017.05.310
15) Khorrami, G.H., Kompany, A., Khorsand Zak, A., 2015. Structural and optical properties of (K,Na)NbO3 nanoparticles synthesized by a modified sol-gel method using starch media. Adv. Powder Technol. 26, 113–118. https://doi.org/10.1016/j.apt.2014.08.013
16) Liu, L., Gao, Z.Y., Su, X.P., Chen, X., Jiang, L., Yao, J.M., 2015. Adsorption removal of dyes from single and binary solutions using a cellulose-based bioadsorbent. ACS Sustain. Chem. Eng. 3, 432–442. https://doi.org/10.1021/sc500848m
17) Mahmood, T., Saddique, M.T., Naeem, A., Westerho, P., Mustafa, S., 2011. Comparison of Different Methods for the Point of Zero Charge Determination of NiO 10017–10023. https://doi.org/10.1021/ie200271d
18) Chen, H.; Wang, L. Nanostructure Sensitization of Transition Metal Oxides for Visible-Light Photocatalysis. *Beilstein J. Nanotechnol.***2014**, *5* (1), 696–710.
19) Tian, N.; Huang, H.; Liu, C.; Dong, F.; Zhang, T.; Du, X.; Yu, S.; Zhang, Y. In Situ Co-Pyrolysis Fabrication of CeO_2 /g-C_3N_4 N–n Type Heterojunction for Synchronously Promoting Photo-Induced Oxidation and Reduction Properties. *J. Mater. Chem. A***2015**, *3* (33), 17120–17129.

20) Malwal, D., Gopinath, P., 2017a. CuO-ZnO Nanosheets with p–n Heterojunction for Enhanced Visible Light Mediated Photocatalytic Activity. ChemistrySelect 2, 4866–4873. https://doi.org/10.1002/slct.201700837
21) Malwal, D., Gopinath, P., 2017b. Efficient adsorption and antibacterial properties of electrospun CuO-ZnO composite nanofibers for water remediation. J. Hazard. Mater. 321, 611–621. https://doi.org/10.1016/j.jhazmat.2016.09.050
22) Malwal, D., Gopinath, P., 2016. Fabrication and applications of ceramic nanofibers in water remediation: A review. Crit. Rev. Environ. Sci. Technol. 46, 500–534. https://doi.org/10.1080/10643389.2015.1109913
23) Mansur, H.S., Sadahira, C.M., Souza, A.N., Mansur, A.A.P., 2008. FTIR spectroscopy characterization of poly (vinyl alcohol) hydrogel with different hydrolysis degree and chemically crosslinked with glutaraldehyde. Mater. Sci. Eng. C 28, 539–548. https://doi.org/10.1016/j.msec.2007.10.088
24) Nasreen, S.A.A.N., Sundarrajan, S., Nizar, S.A.S., Ramakrishna, S., 2019. Nanomaterials: Solutions to water-concomitant challenges. Membranes (Basel). 9, 1–21. https://doi.org/10.3390/membranes9030040
25) Pan, M., Lin, X., Xie, J., Huang, X., 2017. RSC Advances Kinetic , equilibrium and thermodynamic studies for modi fi ed palygorskite nano-composites 4492–4500. https://doi.org/10.1039/c6ra26802a
26) Patiha, Heraldy, E., Hidayat, Y., Firdaus, M., 2016. The langmuir isotherm adsorption equation: The monolayer approach. IOP Conf. Ser. Mater. Sci. Eng. 107. https://doi.org/10.1088/1757-899X/107/1/012067
27) Purushothaman, A.E., Thakur, K., Kandasubramanian, B., 2019. Development of highly porous, Electrostatic force assisted nanofiber fabrication for biological applications. Int. J. Polym. Mater. Polym. Biomater. 0, 1–28. https://doi.org/10.1080/00914037.2019.1581197
28) Puvaneswari, N., Muthukrishnan, J., Gunasekaran, P., 2006. Toxicity assessment and microbial degradation of azo dyes. Indian J. Exp. Biol. 44, 618–26.
29) Tan, Y.N., Wong, C.L., Mohamed, A.R., 2011. An Overview on the Photocatalytic Activity of Nano-Doped- <math><msub><mtext>TiO</mtext><mn mathvariant="bold">2</mn></msub></math> in the Degradation of Organic Pollutants.

ISRN Mater. Sci. 2011, 1–18. https://doi.org/10.5402/2011/261219

30) Teck, C., 2017. Progress in Polymer Science Nanofiber technology : current status and emerging developments. Prog. Polym. Sci. 70, 1–17. https://doi.org/10.1016/j.progpolymsci.2017.03.002

31) Thavasi, V., Singh, G., Ramakrishna, S., 2008. Electrospun nanofibers in energy and environmental applications. Energy Environ. Sci. 1, 205–221. https://doi.org/10.1039/b809074m

32) Yin, M., Wu, C.K., Lou, Y., Burda, C., Koberstein, J.T., Zhu, Y., O'Brien, S., 2005. Copper oxide nanocrystals. J. Am. Chem. Soc. 127, 9506–9511. https://doi.org/10.1021/ja050006u

33) Yu, J., Yu, H., Cheng, B., Zhao, X., Zhang, Q., 2006. Preparation and photocatalytic activity of mesoporous anatase TiO2 nanofibers by a hydrothermal method. J. Photochem. Photobiol. A Chem. 182, 121–127. https://doi.org/10.1016/j.jphotochem.2006.01.022

.